



A Stochastic Theory of Longitudinal Dynamics and Energy Consumption of Road Vehicles

Downloaded from: <https://research.chalmers.se>, 2025-09-25 04:25 UTC


Citation for the original published paper (version of record):

Romano, L., Podgorski, K., Emvin, C. et al (2025). A Stochastic Theory of Longitudinal Dynamics and Energy Consumption of Road Vehicles. IEEE Transactions on Intelligent Vehicles, 10 (3): 1820-1840. <http://dx.doi.org/10.1109/TIV.2024.3435980>

N.B. When citing this work, cite the original published paper.

© 2025 IEEE. Personal use of this material is permitted. Permission from IEEE must be obtained for all other uses, in any current or future media, including reprinting/republishing this material for advertising or promotional purposes, or reuse of any copyrighted component of this work in other works.

A Stochastic Theory of Longitudinal Dynamics and Energy Consumption of Road Vehicles

Luigi Romano , *Member, IEEE*, Krzysztof Podgórski , Carl Emvin , Pär Johannesson , Jonas Fredriksson ,
and Fredrik Bruzelius 

Abstract—Detailed longitudinal dynamics simulations may be used to predict the energy performance of road vehicles. However, including uncertainty in the operating conditions often implies high computational costs. Model-based formulations, in conjunction with statistical methods, may obviate this limitation by directly accounting for stochasticity, thus eliminating the need for simulating large populations of driving and operating cycles. To this end, leveraging directly the methods of stochastic calculus, this work presents a novel theory of longitudinal vehicle dynamics and energy consumption, where the vehicle's speed varies stochastically depending on the characteristics of the operating environment. In particular, the proposed formulation, consisting of stochastic differential equations (SDEs) governing the longitudinal motion of road vehicles, inherently accounts for the statistical variation connected with uncertainties in the driver's behavior and road properties, including, e.g., topography and legal speed. A Fokker-Planck partial differential equation (PDE) that describes the time evolution of the joint probability density function (PDF) of the vehicle's speed, position, and road parameters is also derived from the SDEs established in the paper. The SDE and Fokker-Planck-based approaches enable statistical estimation of important quantities like speed fluctuations, instantaneous power requests, and energy consumption. The developed models may be used to assess the energy performance of road vehicles for different combinations of road transport missions. This is applicable at the early stages of the development, virtual testing, and certification processes, without the need to perform computationally expensive simulations, as corroborated by the virtual experiments conducted in the paper.

Index Terms—Longitudinal vehicle dynamics, stochastic processes, stochastic differential equations, Fokker-Planck equations, energy consumption.

Manuscript received 16 July 2024; accepted 28 July 2024. Date of publication 30 July 2024; date of current version 15 August 2025. The work of Krzysztof Podgórski was supported by the Swedish Research Council (VR) under Grant DNR: 2020-05168. The work of Jonas Fredriksson was supported by the Swedish Electromobility Centre (SEC) and the project Energy Management Strategies for Electrified Vehicles under Traffic Uncertainties under Grant P12057. This work was supported by the Swedish Energy Agency and the Swedish Vehicle Research and Innovation Programme (FFI) through the project U-FEEL under Grant P2022-00948. (*Corresponding author: Luigi Romano.*)

Luigi Romano is with the Department of Electrical Engineering, Linköping University, SE-581 83 Linköping, Sweden (e-mail: luigi.romano@liu.se).

Krzysztof Podgórski is with the Department of Statistics, Lund University, 220 07 Lund, Sweden.

Carl Emvin and Fredrik Bruzelius are with the Department of Mechanical Engineering and Maritime Sciences, Chalmers University of Technology, 41296 Gothenburg, Sweden.

Pär Johannesson is with the Mechanical Research and Innovation Unit, RISE Research Institute of Sweden, 417 56 Gothenburg, Sweden.

Jonas Fredriksson is with the Department of Electrical Engineering, Chalmers University of Technology, 41296 Gothenburg, Sweden.

Color versions of one or more figures in this article are available at <https://doi.org/10.1109/TIV.2024.3435980>.

Digital Object Identifier 10.1109/TIV.2024.3435980

I. INTRODUCTION

THE present Section provides an exhaustive discussion about the research background, formulates the main research questions, and highlights the paper's contributions.

A. Research Motivation and Background

The role played by human activity in climate change, particularly relating to the transport of goods and people, is widely attested by the scientific literature and is now beyond dispute [1], [2], [3], [4], [5], [6], [7], [8], [9], [10]. To mitigate the emissions of pollutants from the transportation sector, the European Commission has prescribed emission thresholds on heavy-duty and passenger vehicles [11], [12], [13], [14]. Preliminary tests to ensure compliance with such limits are carried out either physically or in simulation, by combining virtual representations of the operating environment with simple models for longitudinal dynamics [15], [16]. An emblematic example of a simulation tool frequently used for this purpose is VECTO, whose adoption is mandatory for the certification of heavy-duty vehicles [17]. In this context, before physical prototypes are built, the main performance indicators, including CO₂ emissions, state-of-charge, energy consumption, and maximum power delivered to the wheels, are often evaluated considering a limited number of missions, which are chosen to be representative of a certain typical usage, depending, for example, on geographical or operational features [18], [19], [20], [21].

Different statistical techniques may be employed to appropriately isolate and select reference driving scenarios by gathering and analyzing copious amounts of data collected from instrumented vehicles. Once a few reference missions have been identified, deterministic models of these – predominantly in the form of a so-called *driving cycle* – are then synthesized, which enables assessing the energy performance of road vehicles in virtual environments [22], [23], [24], [25], [26], and testing control and estimation algorithms [27], [28], [29], [30], [31], [32], [33], [34], [35], [36], [37], [38]. On the one hand, by carefully selecting a reduced number of representative scenarios, such an approach has the advantage of avoiding the simulation of large populations of driving cycles, which might be computationally prohibitive; on the other hand, it inevitably leads to excluding any form of statistical uncertainty concerning the modalities by which vehicles are operated on the road [39], [40], [41], [42]. As a consequence, the energy performance and the power request

estimated in simulation rarely coincide with the real one and, in some extreme cases, may even exhibit unacceptably large deviations. A second disadvantage, inherently related to the problem just mentioned above, is that vehicle configurations optimized concerning a single mission may perform relatively poorly when operated in different conditions, which is typically the case in real-world scenarios. Similarly, control algorithms developed and tested using only a scarce number of representative missions may not be robust enough to handle uncovered circumstances.

To obviate these limitations, an alternative description to the conventional driving cycle representation, namely the *operating cycle*, has been recently developed which instead considers explicitly the statistical variation between individual missions [43], [44], [45], [47], [48]. Indeed, the operating cycle utilizes a collection of stochastic models to describe all the relevant factors that may affect the energy performance of road vehicles, including road characteristics [44], but also traffic and weather conditions [45], and mission properties¹ [46]. The main disadvantage connected with the operating cycle representation resides in that, requiring a dynamic model for the longitudinal vehicle motion and driver behavior, is more computationally expensive compared to a driving cycle [50]. Moreover, evaluating the statistical distribution of energy consumption implies the necessity of simulating large populations of synthetic missions, which is also unfeasible when it comes to vehicle design optimization [50], [51].

B. Research Questions

Owing to these premises, it is worth exploring the possibility of predicting directly the energy performance of road vehicles using analytical models in conjunction with the methods of stochastic calculus, as an alternative to simulation. For example, this might be achieved by combining the equations for the longitudinal motion of road vehicles with stochastic processes describing the salient properties of the operating environment, like those collected in the operating cycle. Since, in the deterministic setting, the governing equations of longitudinal vehicle dynamics are ordinary differential equations (ODEs) [15], [16], introducing a stochastic component would in turn provide an alternative representation in terms of stochastic differential equations (SDEs) of diffusion, where the evolution of the vehicle's speed is dictated by that of the stochastic models for the environment, and the driver's control action. Intimately connected to the SDE representation of the longitudinal vehicle dynamics, is the possibility of estimating the probability density function (PDF) and cumulative density function (CDF) of the corresponding physical variables – like, e.g., speed fluctuations, road characteristics, and traveled distance – using a so-called *Fokker-Planck partial differential equation*² (PDE) [53], [54], [55]. Similar approaches, involving combinations of SDEs and related PDEs, are very frequently encountered in fields like physics, chemistry, and econometrics [56], [57], [58], but not

uncommon even in some branches of mechanical engineering, primarily including tribology and contact mechanics [59], [60], [61], [62], [63], where the interest is essentially on the statistics of a certain quantity, rather than its realizations. Regarding instead the longitudinal dynamics of road vehicles, a timid attempt in the same direction was initially made in [64], but, to the best of the authors' knowledge, the potential of a fully stochastic, analytical approach has never been investigated in detail in previous studies.

According to the above discussion, the principal research questions motivating the present paper may be formulated as follows:

- Can the methods of stochastic calculus be combined with the governing equations of longitudinal vehicle dynamics, leading to models formulated directly in terms of SDEs and PDEs, and intrinsically able to capture variation in performance and operating conditions?
- Starting with such SDE and PDE formalisms, is it possible to build a statistical theory of how vehicles move and consume, based on simple yet sound physical principles?

C. Paper's Contributions and Limitations

The present work aims to close the identified research gap by introducing a stochastic approach to longitudinal road vehicle dynamics, combining SDE and PDE-based formalisms. The structure of such equations is deduced from sound first-order physical principles, departing from the commonly accepted formulations found in standard references [15], [16]. Based on these, an approximated, ergodic³ theory of energy consumption is also established, allowing straightforward estimation of vehicular performance. Given the more involved nature of the underlying equations, it should be emphasized that the rigorous analytical treatment of the SDE and PDE formulations proposed in the paper would inevitably necessitate some simplifications compared to the conventional simulation approach.

At the same time, by leveraging directly the methods of stochastic calculus, the original theory proposed in this work has at least two important merits. First, being entirely grounded on physical equations and principles, it permits explaining with simple yet rigorous mathematical models how road vehicles move and consume in a statistical sense. This is a major advantage, especially considering that the models currently available from the literature are purely empirical, with the drawback of lacking a clear physical interpretation [65], [66]. Second, the theory formulated in this paper provides an alternative representation to driving and operating cycles, which does not require simulating detailed vehicle models, and, under favorable circumstances, may even allow for the derivation of closed-form expressions describing the instantaneous power request and energy consumption. In turn, these may conveniently be adopted to support the processes of vehicle design optimization, virtual testing, and certification, as well as the development of robust control algorithms.

¹Originally introduced in [43], [44], the operating cycle format has been brought to full conceptual and mathematical maturity in [47], [48]. Recently, extensions to other types of transport missions have also appeared [49].

²Also known as *Kolmogorov forward equation* [52].

³Such a theory will be referred to as *ergodic* in what follows because it will be essentially grounded on the assumption that the considered stochastic processes satisfy the ergodic hypothesis.

Summarizing, the two main contributions of the paper are:

- The development of a stochastic theory of longitudinal road vehicle dynamics, which is entirely physically motivated and allows for the derivation of both numerical and closed-form solutions,
- The establishment of an approximated statistical theory of energy consumption of road vehicles, representing a computationally inexpensive alternative to driving and operating cycles.

On the other hand, two major limitations of the present work are as follows:

- The effect of powertrain dynamics is disregarded,
- Complex traffic scenarios and driving behaviors are not accounted for.

It is however worth emphasizing that more sophisticated powertrain, traffic, and driver models may easily be accommodated in future extensions of this manuscript, thus overcoming the above limitations. On the other hand, uncertainty is explicitly considered in this paper, since the adopted description of longitudinal vehicle dynamics is stochastic in nature.

D. Paper's Structure

The remainder of the manuscript is organized as follows. Section II introduces the fundamental theory behind the stochastic modeling of longitudinal road vehicle dynamics, along with the SDE and Fokker-Planck-based formalisms. A specific example, considering a proportional-derivative (PD) driver model, in conjunction with an Ornstein-Uhlenbeck process to describe the road topography, is adduced in Section III, where some closed-form results are also derived. The ergodic theory of energy consumption is then established in Section IV, based on the preliminary results obtained in Section III. The theoretical predictions are validated against simulations conducted in VehProp [50], [67], a higher-fidelity environment for studies concerned with longitudinal vehicle dynamics and energy consumption. Finally, the paper terminates with an extended discussion in Section V, where the main conclusions are drawn and an outlook for future research is given. Some additional analytical results are more conveniently collected in Appendix A. A concluding note: although this work aims to present the main results in a rigorous, sound mathematical way, the focus is predominantly on their physical interpretation, and often closed-form solutions will be privileged over results of a more general nature. This is also the main reason for which the proposed approach is elucidated using relatively simple models: the adoption of more sophisticated formulations to describe the vehicle, driver, and environment would preclude the derivation of analytical expressions that are instead indispensable to grasp the salient features of the theory, with the risk of obscuring some important arguments in favor of generality.

II. THEORETICAL DEVELOPMENT

The present section is dedicated to the development of a general, stochastic theory of longitudinal road vehicle dynamics. Two formalisms are presented in Sections II-B and II-C, respectively: the SDE-based representation and its Fokker-Planck

counterpart. Both approaches allow to estimate the statistical properties of certain quantities in interest – comprising primarily the vehicle's speed and the road characteristics – which are necessary to analyze energy performance indicators.

A. Preliminaries and Notation

In this paper, the notation is as follows: the set of real numbers is indicated with \mathbb{R} ; the sets of positive real numbers is denoted by $\mathbb{R}_{\geq 0}$ when including the zero and by $\mathbb{R}_{> 0}$ when excluding it. The set of positive integer numbers is indicated with \mathbb{N} , whereas \mathbb{N}_0 denotes the extended set of positive integers including zero, i.e., $\mathbb{N}_0 = \mathbb{N} \cup \{0\}$. A continuous-time, vector-valued stochastic process is denoted by $\{\mathbf{A}(t)\}_{t \in [t_0, t_F]}$ for $t \in [t_0, t_F]$, being $t_0 < t_F \in \mathbb{R}_{\geq 0}$. Similarly, a discrete-time, vector-valued stochastic process is indicated by $\{\mathbf{A}_k\}_{k \in \mathbb{N}_0}$. A complete probability space is denoted by $(\Omega, \mathcal{F}, \mathbb{P})$, where Ω represents the sample space, \mathcal{F} the σ -algebra, and \mathbb{P} the probability measure; a filtered probability space, with filtration generated by a stochastic process $\{\mathbf{A}(t)\}_{t \in [t_0, t_F]}$, is indicated with $(\Omega, \mathcal{F}, \mathbb{F}_{\mathbf{A}}, \mathbb{P})$, where $\mathcal{F}_{\mathbf{A}}(t) = \sigma(\{\mathbf{A}(t')\}_{t' \in [t_0, t]})$, and $\mathbb{F}_{\mathbf{A}} = \{\mathcal{F}_{\mathbf{A}}(t)\}_{t \in [t_0, t_F]}$. The probability and expectation operators are denoted as $\mathbb{P}(\cdot)$ and $\mathbb{E}(\cdot)$, respectively; variance and covariance as $\text{Var}(\cdot)$ and $\text{Cov}(\cdot)$. For a generic random variable (or process) \mathbf{A} , the corresponding lowercase letter \mathbf{a} denotes its realization, i.e., the value of $\mathbf{A}(\omega)$ at the specific $\omega \in \Omega$. For a scalar process $\{A(t)\}_{t \in [t_0, t_F]}$, the time-varying quantities $\mu_A(t)$ and $\sigma_A(t)$, $t \in [t_0, t_F]$, are the mean and variance of $A(t)$, respectively. For a generic function $f(\cdot)$, the limit $\lim_{t \rightarrow \infty} f(t)$, when exists, is often abbreviated as $f(\infty)$ for ease of notation. Indicator functions are denoted by $\mathbb{1}_{a \in \mathcal{A}}$ and assume a value of one if $a \in \mathcal{A}$ and zero otherwise. Finally, the symbol $\|\cdot\|$ represents a norm (usually, the Euclidean norm) on a finite-dimensional space.

B. Stochastic Longitudinal Vehicle Dynamics

In the foundation of a stochastic theory of energy consumption, the first and most important step consists of deriving the SDE system governing the longitudinal vehicle dynamics and the evolution of the related road characteristics. To this end, consider the equation of motion for the longitudinal dynamics of a road vehicle [15], [16]:

$$m^* \dot{v}(t) = F_x(v(t), \dot{v}(t), w(t), \zeta(t), t) + F_{\text{ext}}(v(t), \zeta(t)), \quad t \in (t_0, t_F), \quad (1)$$

where the state $v(t) \in \mathbb{R}_{\geq 0}$ is the vehicle's velocity, $t \in [t_0, t_F]$ is the independent time variable, m^* denotes the augmented mass of the vehicle, incorporating the inertial contributions originating from the rotating components, the propulsive force $F_x(v(t), \dot{v}(t), w(t), \zeta(t), t) \in \mathbb{R}$ may be computed as the torque reduced at the wheel level, under the assumption of no-slip conditions, $w(t) \in \mathbb{R}$ represents a one-dimensional Gaussian white noise⁴, and the term $F_{\text{ext}}(v(t), \zeta(t)) \in \mathbb{R}$ includes all the

⁴More complex structures for the noise term might be chosen, at the cost of rendering the mathematical analysis much more involved.

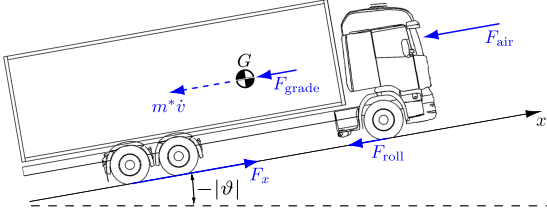


Fig. 1. Longitudinal equilibrium of a rigid truck driving uphill. The total external force acting in the longitudinal direction, $F_{\text{ext}} = F_{\text{grade}} + F_{\text{roll}} + F_{\text{air}}$, consists of the longitudinal component of the gravity force due to the road inclination angle ϑ , $F_{\text{grade}} = mg \sin \vartheta$, the rolling resistance force $F_{\text{roll}} = -f_r mg \cos \vartheta$, and the air resistance $F_{\text{air}} = -\frac{1}{2} \rho_{\text{air}} C_d A_f v^2$, also called aerodynamic resistance or air drag. The total inertial force $F_{\text{inertia}} = -m^* \dot{v}$ (dashed line) accounts for the contributions relating to the rotating components, under the assumption of no slip-conditions.

external forces acting on the vehicle, depending on a certain set of given quantities $\zeta(t) \in \mathbb{R}^{n_\zeta}$ to be properly defined. For instance, as graphically illustrated in Fig. 1, a possible expression for the external forces $F_{\text{ext}}(v(t), \zeta(t))$ might be

$$F_{\text{ext}}(v(t), \zeta(t)) = mg \sin \vartheta(t) - f_r mg \cos \vartheta(t) - \frac{1}{2} \rho_{\text{air}} C_d A_f v^2(t), \quad (2)$$

or, considering small road inclination angles $\vartheta(t) \in [-\pi/2, \pi/2]$, that is, approximating $\sin \vartheta(t) \approx \vartheta(t)$ and $\cos \vartheta(t) \approx 1$,

$$F_{\text{ext}}(v(t), \zeta(t)) = mg \vartheta(t) - f_r mg - \frac{1}{2} \rho_{\text{air}} C_d A_f v^2(t). \quad (3)$$

In both (2) and (3), m denotes the actual mass of the vehicle, f_r is the rolling resistance coefficient, which may be supposed constant for simplicity, ρ_{air} denotes the air density, C_d the drag coefficient and A_f the vehicle's frontal area. Equations (2) and (3) constitute two prototypical examples of common expressions found in the literature dedicated to longitudinal vehicle dynamics [15], [16]; more refined formulations, considering, e.g., secondary effects connected to curvature and high lateral accelerations, which are deliberately ignored in the present paper, may instead be found in [68], [69] (for further details involving this example and a specification of $\zeta(t)$, see Section III).

In any case, by opportunely prescribing the analytical expressions for $F_x(v(t), \dot{v}(t), w(t), \zeta(t), t)$ and $F_{\text{ext}}(v(t), \zeta(t))$, and possibly after performing a change of variables, it may be postulated that (1) admits a state-space representation in the form

$$\dot{v}(t) = f(v(t), w(t), \zeta(t), t), \quad t \in (t_0, t_F), \quad (4)$$

where $f(v(t), w(t), \zeta(t), t)$ is a function of the state, the one-dimensional white noise, the time, and eventually the variables $\zeta(t)$. The latter may include, for example, parameters related to road properties, or to control actions required by the driver, even though their specification is not essential at this stage. Instead, the key assumption made in the following is that, conditional to a given road segment, the physical variables considered in (4) only produce small fluctuations of the velocity $\tilde{v}(t) \triangleq v(t) - v^*$ around the stationary value v^* . On a homogeneous road segment,

such value is assumed to coincide with a desired speed chosen by the driver depending on certain road or traffic parameters like, e.g., legal speed, road curvature, or traffic density. This modeling approach is consistent with the hypothesis that the driver's behavior may be separated into a tactical and operational part: the former interprets the stimuli relating to quantities that do not appear explicitly in (1), and is responsible for setting a reference speed; the latter, on the other hand, models the driver's reaction to the external perturbations that explicitly show in the equations of motion [43]. From a purely mathematical perspective, it should be clarified that the introduction of a stationary speed v^* is not essential for the derivation of the governing SDEs of longitudinal vehicle dynamics; however, it enormously simplifies the treatment, being also propaedeutic for the development of the approximated theory of energy consumption presented in Section IV.

Owing to these premises, on each road segment, (4) may be linearized according to

$$\begin{aligned} \dot{\tilde{v}}(t) &= \tilde{f}(\tilde{v}(t), w(t), \zeta(t), t | v^*) \triangleq f(v^*, w(t), \zeta(t), t) \\ &+ \left. \frac{\partial f(v(t), w(t), \zeta(t), t | v^*)}{\partial v} \right|_{v=v^*} \tilde{v}(t), \quad t \in (t_0, t_F), \end{aligned} \quad (5)$$

where the new notation has been introduced to distinguish between the actual variables and the constant velocity v^* , interpreted henceforth as a conditional parameter.

By performing the change of variable $ds = v(t)dt \approx v^*dt$, with some abuse of notation, (5) may be then converted into

$$\frac{d\tilde{v}(s)}{ds} = \tilde{f}(\tilde{v}(s), w(s), \zeta(s), s | v^*), \quad s \in (s_0, s_F). \quad (6)$$

The representation adopted in (6) is more convenient than that in (5), since some of the quantities collected in the vector ζ are usually modeled explicitly as functions of the traveled distance s rather than the time t , i.e., $\zeta = \zeta(s)$ (to realize this, it may suffice to think of road characteristics like topography and sequences of speed limits, which occupy fixed positions along the road).

At this point, it may be postulated that the set of variables $\zeta(s)$ admits a decomposition of the type $\zeta(s) = (\zeta^*, z(s)) \in \mathbb{R}^{n_{\zeta^*}} \times \mathbb{R}^{n_z}$, where $\zeta^* \in \mathbb{R}^{n_{\zeta^*}}$ consists of those parameters which may be regarded as conditionally constant over the given road segment, whereas $z(s) \in \mathbb{R}^{n_z}$ models the quantities that vary over traveled distance. More specifically, inspired by the formulations proposed in [43], [47], [48], it is supposed in the present paper that these behave stochastically. Therefore, $z(s)$ is interpreted as a realization of the stochastic process $Z(s) \in \mathbb{R}^{n_z}$, which satisfies a system of SDEs of diffusion:

$$dZ(s) = \alpha(Z(s), s | \zeta^*)ds + \sigma(Z(s), s | \zeta^*)dB_Z(s), \quad s \in (s_0, s_F), \quad (7)$$

where $B_Z(s) \in \mathbb{R}^{n_{BZ}}$ denotes a multi-dimensional Brownian motion (also known as Wiener process), and the coefficients $\alpha(Z(s), s | \zeta^*) \in \mathbb{R}^{n_z}$, $\sigma(Z(s), s | \zeta^*) \in \mathbb{R}^{n_z \times n_{BZ}}$ may generally be time-varying and stochastic (it follows from (7) that the process $\{Z(s)\}_{s \in [s_0, s_F]}$ is adapted to the natural

filtration $(\Omega, \mathcal{F}, \mathbb{F}_{B_Z}, \mathbb{P})$ generated by the Brownian motion $\{\mathbf{B}_Z(s)\}_{s \in [s_0, s_F]}$.

Since the dynamics of the parameters $\mathbf{Z}(s)$ are governed by a possibly vector-valued SDE, and assuming reasonably that $\tilde{f}(\tilde{v}(s), w(s), \zeta(s), s | v^*)$ be linear in $w(t)$, the equation of motion (1) also becomes stochastic, according to

$$\begin{aligned} d\tilde{V}(s) &= \tilde{g}(\tilde{V}(s), \mathbf{Z}(s), s | v^*, \zeta^*) ds \\ &+ \tilde{h}(\tilde{V}(s), \mathbf{Z}(s), s | v^*, \zeta^*) dB_{\tilde{V}}(s), \quad s \in (s_0, s_F), \end{aligned} \quad (8)$$

where, again with a slight abuse of notation, the variables ζ^* are treated as conditional parameters, and $dB_{\tilde{V}}(s) \triangleq v^* w(s) ds$, being $B_{\tilde{V}}(s)$ another Brownian motion which is supposed to be independent of $\mathbf{B}_X(s)$.

Equations (7) and (8) may be finally combined together yielding a system of SDEs of diffusion describing the stochastic evolution of the speed fluctuation $\tilde{V}(s)$ depending on that of the physical variables $\mathbf{Z}(s)$. More specifically, by introducing $\mathbb{R}^{n_X} \triangleq \mathbb{R}^{n_Z+1}$, $\mathbb{R}^{n_{B_X}} \triangleq \mathbb{R}^{n_{B_Z}+1}$, $\mathbb{R}^{n_{\xi^*}} \triangleq \mathbb{R}^{n_{\zeta^*}+1}$ for convenience of notation, and defining accordingly the vectors $\mathbb{R}^{n_X} \ni \mathbf{X}(s) \triangleq [\mathbf{Z}(s)^T \tilde{V}(s)]^T$, $\mathbb{R}^{n_{B_X}} \ni \mathbf{B}_X(s) \triangleq [\mathbf{B}_Z(s)^T B_{\tilde{V}}(s)]^T$, $\mathbb{R}^{n_{\xi^*}} \ni \xi^* \triangleq (\zeta^*, v^*)$, and $\mathbb{R}^{n_X} \ni \gamma(\mathbf{X}(s), s | \xi^*) \triangleq [\alpha^T(\mathbf{Z}(s), s | \xi^*) \tilde{g}(\mathbf{X}(s), s | \xi^*)]^T$, and the matrix $\mathbb{R}^{n_X \times n_{B_X}} \ni \omega(\mathbf{X}(s), s | \xi^*)$ as

$$\omega(\mathbf{X}(s), s | \xi^*) \triangleq \begin{bmatrix} \sigma(\mathbf{Z}(s), s | \xi^*) & \mathbf{0} \\ \mathbf{0} & \tilde{h}(\mathbf{X}(s), s | \xi^*) \end{bmatrix}, \quad (9)$$

the SDE system described by (7) and (8) may be restated more compactly in the form

$$d\mathbf{X}(s) = \gamma(\mathbf{X}(s), s | \xi^*) ds + \omega(\mathbf{X}(s), s | \xi^*) d\mathbf{B}_X(s), \quad s \in (s_0, s_F), \quad (10)$$

which is a vector-valued SDE coupling the speed perturbation dynamics to those of the road and mission parameters. The SDE system above might generally be nonlinear but, under opportune assumptions on the drift and diffusion terms $\gamma(\mathbf{X}(s), s | \xi^*)$, and $\omega(\mathbf{X}(s), s | \xi^*)$, respectively, as well as on the initial conditions (ICs), existence and uniqueness would follow from standard arguments [70], [71].

C. Fokker-Planck Equation

Equation (10) allows reinterpreting the stochastic longitudinal problem according to the equivalent Fokker-Planck formulation [55], which specifically yields the following PDE:

$$\begin{aligned} \frac{\partial p(\mathbf{x}, s | \xi^*)}{\partial s} &= - \sum_{i=1}^{n_X} \frac{\partial}{\partial x_i} \left[\gamma_{X_i}(\mathbf{x}, s | \xi^*) p(\mathbf{x}, s | \xi^*) \right] \\ &+ \sum_{i,j=1}^{n_X} \frac{\partial^2}{\partial x_i \partial x_j} \left[D_{X_i X_j}(\mathbf{x}, s | \xi^*) p(\mathbf{x}, s | \xi^*) \right], \\ (\mathbf{x}, s) &\in \mathbb{R}^{n_X} \times (s_0, s_F), \end{aligned} \quad (11)$$

where the coefficients $D_{X_i X_j}(\mathbf{x}, s | \xi^*)$, $i, j \in \{1, \dots, n_X\}$, denote the entries of the diffusion tensor, given by $\mathbb{R}^{n_X \times n_X} \ni \mathbf{D}(\mathbf{x}, s | \xi^*) \triangleq \frac{1}{2} \omega(\mathbf{x}, s | \xi^*) \omega^T(\mathbf{x}, s | \xi^*)$. In (11), the unknown quantity $p(\mathbf{x}, s | \xi^*)$ represents the multivariate PDF for the vector-valued random variables appearing in (10), conditional to a given set of parameters ξ^* . If these are, in turn, interpreted as random variables Ξ^* , then⁵

$$\begin{aligned} p(\mathbf{x}, s | \xi^*) &\triangleq f_{\mathbf{X}(s) | \Xi^*}(\mathbf{x}, s | \xi^*) \\ &= \mathbb{P}(\mathbf{X}(s) = \mathbf{x} | \Xi^* = \xi^*). \end{aligned} \quad (12)$$

In particular, by enforcing a general initial condition (IC) of the type

$$p(\mathbf{x}, s_0 | \xi^*) = \delta(\mathbf{x} - \mathbf{x}_0), \quad (13)$$

with $\delta(\cdot)$ indicating the Dirac distribution, any solution to the Fokker-Planck (11) would yield the transition probability $p(\mathbf{x}, s | \mathbf{x}_0, s_0, \xi^*)$ for $s \in (s_0, s_F)$ [55], [72], i.e., formally

$$\begin{aligned} p(\mathbf{x}, s | \mathbf{x}_0, s_0, \xi^*) &= f_{\mathbf{X}(s) | \mathbf{X}(s_0), \Xi^*}(\mathbf{x}, s | \mathbf{x}_0, s_0, \xi^*) \\ &= \mathbb{P}(\mathbf{X}(s) = \mathbf{x} | \mathbf{X}(s_0) = \mathbf{x}_0, \Xi^* = \xi^*). \end{aligned} \quad (14)$$

D. Stochastic Power, Energy, and Energy Consumption

The knowledge of the stochastic road characteristics, together with that of the speed perturbations, is crucial in determining the statistical properties of performance indicators like propulsive power and energy consumption.

For a deterministic system, neglecting the term relating to the (usually small) additive white noise, the power delivered to the wheels, conditional to a given road segment, may be computed accordingly as

$$\begin{aligned} P_d(s | \xi^*) &= \max \left\{ 0, F_x(v(s), \dot{v}(s), \zeta(s), s) \right\} v(s) \\ &= \max \left\{ 0, \tilde{F}_x(\mathbf{x}(s), s | \xi^*) \right\} v(s) \\ &\approx \max \left\{ 0, \tilde{F}_x(\mathbf{x}(s), s | \xi^*) \right\} v^*, \quad s \in (s_0, s_F), \end{aligned} \quad (15)$$

where evidently

$$\begin{aligned} \tilde{F}_x(\mathbf{x}(s), s | \xi^*) &\triangleq F_x(v(s), \dot{v}(s), \zeta(s), s) \Big|_{v(s)=v^*+\tilde{v}(s), \dot{v}(s)=\tilde{f}(\tilde{v}(s), \zeta(s), s | v^*)} \\ &= F_x(v(s), \dot{v}(s), \zeta(s), s) \Big|_{v(s)=v^*+\tilde{v}(s), \dot{v}(s)=\tilde{f}(\tilde{v}(s), \zeta(s), s | v^*)}. \end{aligned} \quad (16)$$

Thus, by treating the velocity fluctuations $\tilde{V}(s)$ and the physical quantities $\mathbf{Z}(s)$ as stochastic variables, the corresponding random power is formally given by

$$\tilde{P}_d(s) \approx \max \left\{ 0, \tilde{F}_x(s) \right\} v^*, \quad s \in (s_0, s_F), \quad (17)$$

⁵It should be observed that the first expression on the right-hand side of (12) considers, in fact, the case of continuous density, whereas the second one replaces the density with the probability in the discrete case. This consideration also applies to (14).

where now $\{\tilde{F}_x(s)\}_{s \in [s_0, s_F]}$ and $\{\tilde{P}_d(s)\}_{s \in [s_0, s_F]}$ are regarded as stochastic processes. Over each road segment, the stochastic energy required to travel a total distance $\Delta s = s_F - s_0 \triangleq v^*(t_F - t_0)$ may hence be calculated as

$$\tilde{E}_d(s_F) \approx \frac{1}{v^*} \int_{s_0}^{s_F} \tilde{P}_d(s) ds, \quad (18)$$

and the energy consumption, that is, the energy consumed per unit of distance, reads accordingly

$$\tilde{e}_d(s_F) \approx \frac{1}{\Delta s} \tilde{E}_d(s_F) \approx \frac{1}{v^*(s_F - s_0)} \int_{s_0}^{s_F} \tilde{P}_d(s) ds. \quad (19)$$

Using the above formulae (17), (18), and (19), the statistical moments of the propulsive power, energy, and energy consumption may be calculated either analytically (when possible), or numerically. The computation would be naturally limited to the considered road segment, characterized by a specific set of parameters ξ^* . However, if on each road segment the stochastic processes in (10), (17), (18), and (19) are, in a certain sense, ergodic and stationary, then their statistical properties might be determined using the standard formulae for the total probability, expectation, and variance. Opportunely supplemented with the ergodic hypothesis, this argument is foundational for the establishment of an approximated stochastic theory of energy consumption, which task is carried out in Section IV leading to the derivation of certain mixture models for the quantities in interest. In this context, it is also worth mentioning that the quantity $\tilde{e}_d(s_F)$ in (19) is proportional to the time average of the stochastic power $\tilde{P}_d(s)$.

III. AN EXAMPLE WITH A PROPORTIONAL-DERIVATIVE DRIVER CONTROLLER AND AN ORNSTEIN-UHLENBECK TOPOGRAPHY MODEL

The present section elucidates the theory outlined above by adducing an example with a proportional-derivative (PD) driver controller, in conjunction with an Ornstein-Uhlenbeck process to describe the road grade. Indeed, apart from allowing explicit analytical solutions, this modeling approach is quite common and has been adopted in previous studies dealing with longitudinal vehicle dynamics [47], [48]. In what follows, the investigation is also restricted to homogeneous road sections, on which the parameters ξ^* may be fairly supposed to be constant. Therefore, to alleviate the notation, the explicit dependency upon the set of parameters ξ^* is omitted, since all the quantities will be conditional to a certain given realization.

The main assumptions and hypotheses behind the subsequent analysis are stated in the next Section III-A. Moreover, whilst Section III-B focuses exclusively on the SDE and Fokker-Planck-based representations, results concerning the statistical distributions of the energy performance indicators are reported in Section III-C.

A. Model Assumptions

In order to derive the stochastic equation for the longitudinal vehicle dynamics, the term $F_x(v(s), \dot{v}(s), w(s), \zeta(s), s)$ is first

modeled by assuming that the driver behaves as a PD controller⁶ with additive white noise. Expressing all the involved quantities in the time domain for convenience gives

$$F_x(v(t), \dot{v}(t), w(t), \zeta(t), t) = k_P(v^* - v(t)) - k_D \dot{v}(t) + k_N w(t). \quad (20)$$

It is worth emphasizing that, albeit being overall quite realistic, the choice of modeling the propulsive force $F_x(v(s), \dot{v}(s), w(s), \zeta(s), s)$ using a PD controller is essentially justified by its simplicity; a generalized model considering a proportional-integral-derivative (PID) controller is however presented in Appendix A. Whilst other driver models be more adequate under certain circumstances [74], [75], [76], [77], [78], the PD (or PID) formulation is preferred in this paper since it permits deriving simple closed-form solutions, and can easily emulate the operational part of the driver model implemented in VehProp⁷, which is used later for validation. Moreover, PD and PID driver controllers are frequently encountered in works concerned with vehicle dynamics [79], [80], [81], [82], [83], and have also been employed in previous studies dealing with operating and driving cycles, showing a good agreement with experimental data and simulations performed in VECTO [44], [64]. Defining

$$\gamma \triangleq \frac{k_P + \rho_{\text{air}} C_d A v^*}{v^*(m^* + k_D)}, \quad (21a)$$

$$\tilde{m} \triangleq \frac{m}{v^*(m^* + k_D)}, \quad (21b)$$

$$\tilde{A}_f \triangleq \frac{A_f}{m^* + k_D}, \quad (21c)$$

$$\eta \triangleq \frac{k_N}{m^* + k_D}, \quad (21d)$$

adopting the simplified expression for the external forces as in (3), recalling that the white noise is formally the (distributional) derivative of the Brownian motion and that, by assumption, $v(t) = v^* + \tilde{v}(t)$, the longitudinal equation of motion may be derived to be of the same form of (6), with

$$\begin{aligned} \tilde{f}(\tilde{v}(s), w(s), \zeta(s), s; v^*) &\triangleq -\gamma \tilde{v}(s) + \tilde{m} g \chi y(s) - f_r \tilde{m} g \\ &\quad - \frac{1}{2} \rho_{\text{air}} C_d \tilde{A}_f v^* + \eta w(s). \end{aligned} \quad (22)$$

In the above (22), $y(s) = \theta(s)/\chi$ denotes the road grade (expressed in percentage), $\chi = 1/100$ is a conversion constant, and the road parameters may be defined as $\zeta^* \triangleq (\gamma, \eta, \tilde{m}, g, f_r, \rho_{\text{air}}, C_d, \tilde{A}_f, k_P, k_D)$.

⁶This formulation is also appropriate to model cruise controllers for partly automated vehicles [73]. In the same context, it is perhaps worth mentioning that PID controllers qualify amongst the simplest ones, whereas nonlinear driver control models may also be adopted, such as those discussed in [38].

⁷In VehProp, the driver model is separated into a tactical and an operational module. The latter is responsible for controlling the acceleration and brake pedal positions, based on the input from the tactical part. See [50], [67] for further details.

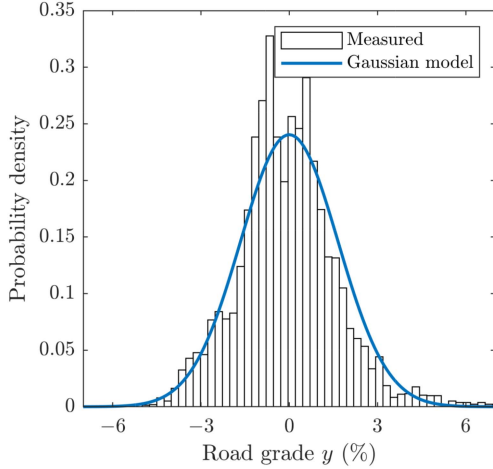


Fig. 2. Comparison between the distribution of the measured road grade for a transport mission taking place in the region of Västra Götaland, Sweden [47], [48], and the analytical pdf of the stationary Ornstein-Uhlenbeck process described by (23) ($Y(\infty) \sim \mathcal{N}\left(0, \frac{\beta^2}{2\alpha}\right)$). More refined, non-Gaussian and non-stationary models for the road topography parameter have been presented in [84], [85].

Concerning the stochastic modeling of the road characteristics, only the topography parameter is considered in the following⁸. In particular, in the discrete setting, the road grade has traditionally been described using either Gaussian or generalized Laplace models [84], [85]. The most common Gaussian model encountered in the literature dealing with longitudinal vehicle dynamics, a first-order, stationary, and ergodic autoregressive (abbreviated AR(1)) process [47], [48], is adopted in this paper for convenience. In fact, apart from its mathematical simplicity, this choice is also motivated by the fact that the nice Gaussian and ergodic properties of the AR(1) model will be automatically transferred to the resulting SDE system (10), owing to the additional assumptions on the driver's behavior⁹. In the continuous setting, the AR(1) formulation is equivalent to an Ornstein-Uhlenbeck process [86], according to

$$dY(s) = -\alpha Y(s)ds + \beta dB_Y(s), \quad s \in (s_0, s_F), \quad (23)$$

with $\alpha, \beta \in \mathbb{R}_{>0}$. Exactly as its discrete counterpart, and under opportune assumptions, an Ornstein-Uhlenbeck process is a stationary Gaussian process with continuous paths $\{Y(s)\}_{s \in [s_0, s_F]}$, and enjoying ergodic properties, as briefly discussed also in the next Section III-B1 and III-B2, respectively. Over relatively short road segments, it captures satisfactorily the behavior of the topography parameter, as also corroborated by empirical evidence in [84], [85] (where the equivalent AR(1) formalism was adopted). In the same context, Fig. 2 shows a comparison between the normal distribution of the Ornstein-Uhlenbeck process obeying (23) and that of the road grade estimated for a

⁸Actually, even the most advanced driving cycles *only* include the road grade concerning the road parameters, whereas other quantities are explicitly considered in the alternative operating cycle representation [47], [48].

⁹It is perhaps worth specifying that the same properties will also be preserved when considering a PID driver model, as done later in Appendix A.

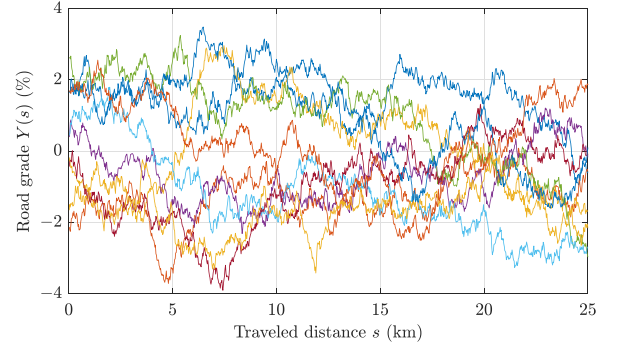


Fig. 3. Ten different sample paths of the Ornstein-Uhlenbeck process describing the road topography parameter according to the SDE (23). All the paths have been generated considering zero initial conditions $Y_0 = Y(s_0) = 0$, and over a total distance of $\Delta s = s_F - s_0 = 25$ km. The values for the parameters $\alpha = 9.16 \cdot 10^{-5} \text{ m}^{-1}$ and $\beta = 0.021 \text{ m}^{-1/2}$ are typical of highway sections in the region of Västra Götaland, Sweden.

single road transport mission taking place in the region of Västra Götaland, Sweden [47], [48].

The relationships between the parameters of the Ornstein-Uhlenbeck processes and those of model presented in [84], [85] may be deduced by observing that an AR(1) process is indeed a discretization of (23) for every possible choice of sampling length. For completeness, Fig. 3 illustrates ten different sample paths (that is, road grade profiles) obtained by simulating the Ornstein-Uhlenbeck process according to (23).

B. Stochastic Longitudinal Vehicle Dynamics and Fokker-Planck Equation

As already mentioned, the true core of the stochastic theory developed in the paper is represented by the SDE system (10) governing the longitudinal dynamics of road vehicles, and its equivalent Fokker-Planck formalism (11). The present section delivers closed-form results derived from the assumption that the road grade and driver model behave as an Ornstein-Uhlenbeck process and a PD controller, respectively.

1) *SDE system for longitudinal vehicle dynamics*: Following the general theory presented in Section II-B, the continuous-time interpretation of the road grade $Y(s)$ in (23) implies that the original ODE for the longitudinal vehicle dynamics also becomes a SDE. Consequently, the two equations may be combined as follows:

$$dY(s) = -\alpha Y(s)ds + \beta dB_Y(s), \quad (24a)$$

$$d\tilde{V}(s) = \left(-\gamma \tilde{V}(s) + \tilde{m}g\chi Y(s) - f_r \tilde{m}g - \frac{1}{2} \rho_{\text{air}} C_d \tilde{A}_f v^* \right) ds + \eta dB_{\tilde{V}}(s), \quad s \in (s_0, s_F). \quad (24b)$$

In vector notation, the SDE system described by (24) may be reformulated as

$$d\mathbf{X}(s) = \mathbf{\Gamma}(\boldsymbol{\theta} - \mathbf{X}(s))ds + \boldsymbol{\omega}d\mathbf{B}_{\mathbf{X}}(s), \quad s \in (s_0, s_F), \quad (25)$$

with

$$\mathbf{\Gamma} = \begin{bmatrix} \gamma_{YY} & \gamma_{Y\tilde{V}} \\ \gamma_{\tilde{V}Y} & \gamma_{\tilde{V}\tilde{V}} \end{bmatrix} \triangleq \begin{bmatrix} \alpha & 0 \\ -\tilde{m}g\chi & \gamma \end{bmatrix}, \quad (26a)$$

$$\boldsymbol{\theta} = \begin{bmatrix} \theta_Y \\ \theta_{\tilde{V}} \end{bmatrix} \triangleq -\frac{1}{\gamma} \begin{bmatrix} 0 \\ f_r \tilde{m}g + \frac{1}{2} \rho_{\text{air}} C_d \tilde{A}_f v^* \end{bmatrix}, \quad (26b)$$

$$\boldsymbol{\omega} = \begin{bmatrix} \omega_{YY} & \omega_{Y\tilde{V}} \\ \omega_{\tilde{V}Y} & \omega_{\tilde{V}\tilde{V}} \end{bmatrix} \triangleq \begin{bmatrix} \beta & 0 \\ 0 & \eta \end{bmatrix}. \quad (26c)$$

The SDEs above, describing a vector-valued Ornstein-Uhlenbeck process, have clearly the same structure of the more general (10), and admit a unique strong solution, with continuous paths and adapted to the filtration $(\Omega, \mathcal{F}, \mathbb{F}_{\mathbf{B}_X}, \mathbb{P})$, for all ICs $\mathbf{X}_0 \triangleq \mathbf{X}(s_0)$ independent of the σ -algebra generated by $\{\mathbf{B}_X(s)\}_{s \in [s_0, s_F]}$, and satisfying additionally $\mathbb{E}(\|\mathbf{X}_0\|^2) < \infty$ (see, e.g., Theorem 6.30 in [70] or Theorem 5.2.1 in [71]). In fact, since the SDE system (25) is linear, its strong solution may be recovered in closed form as follows:

$$\begin{aligned} \mathbf{X}(s) &= e^{-\mathbf{\Gamma}(s-s_0)} \mathbf{X}_0 + \left(\mathbf{I} - e^{-\mathbf{\Gamma}(s-s_0)} \right) \boldsymbol{\theta} \\ &+ \int_{s_0}^s e^{-\mathbf{\Gamma}(s-s')} \boldsymbol{\omega} d\mathbf{B}_X(s'), \quad s \in [s_0, s_F], \end{aligned} \quad (27)$$

with the matrix exponential reading specifically

$$e^{-\mathbf{\Gamma}s} = \begin{bmatrix} e^{-\alpha s} & 0 \\ \frac{\tilde{m}g\chi(e^{-\alpha s} - e^{-\gamma s})}{\gamma - \alpha} & e^{-\gamma s} \end{bmatrix}. \quad (28)$$

The continuity of the paths of $\{\mathbf{X}(s)\}_{s \in [s_0, s_F]}$ may be inferred directly from the representation formula (27). The peculiar expression for the matrix exponential $e^{-\mathbf{\Gamma}s}$ as in the above (28) is a consequence of the fact that, as already anticipated, the dynamics of the road grade $Y(s)$ are independent of those of the speed fluctuations $\tilde{V}(s)$, due to the cascaded structure of the SDE system (25).

As for its one-dimensional counterpart, the Ornstein-Uhlenbeck process (25) is Gaussian, and therefore completely characterized by its mean $\boldsymbol{\mu}(s | \mathbf{x}_0, s_0)$ and covariance matrix $\boldsymbol{\Sigma}(s - s_0)$, conditional to $\mathbf{X}(s_0) = \mathbf{x}_0$. In particular, from the analytical solution (27) and invoking Itô's Lemma, the following expressions may be deduced, respectively,

$$\begin{aligned} \boldsymbol{\mu}(s | \mathbf{x}_0, s_0) &= \mathbb{E}(\mathbf{X}(s) | \mathbf{X}(s_0) = \mathbf{x}_0) \\ &= e^{-\mathbf{\Gamma}(s-s_0)} \mathbf{x}_0 + \left(\mathbf{I} - e^{-\mathbf{\Gamma}(s-s_0)} \right) \boldsymbol{\theta}, \end{aligned} \quad (29a)$$

$$\begin{aligned} \boldsymbol{\Sigma}(s) &= \text{Cov}(\mathbf{X}(s), \mathbf{X}(s)) \\ &= \int_0^s e^{-\mathbf{\Gamma}s'} \boldsymbol{\omega} \boldsymbol{\omega}^T e^{-\mathbf{\Gamma}^T s'} ds', \end{aligned} \quad (29b)$$

being the latter quantity clearly independent of the IC $\mathbf{X}(s_0) = \mathbf{x}_0$ [55], [72], [87]. Whilst the analytical expression for the mean $\boldsymbol{\mu}(s | \mathbf{x}_0, s_0) = [\mu_Y(s | \mathbf{x}_0, s_0) \ \mu_{\tilde{V}}(s | \mathbf{x}_0, s_0)]^T$ may be easily obtained by combining the expressions in (26) and (28), the

entries of the time-dependent covariance matrix $\boldsymbol{\Sigma}(s)$, given by

$$\boldsymbol{\Sigma}(s) = \begin{bmatrix} \Sigma_{YY}(s) & \Sigma_{Y\tilde{V}}(s) \\ \Sigma_{\tilde{V}Y}(s) & \Sigma_{\tilde{V}\tilde{V}}(s) \end{bmatrix}, \quad (30)$$

read according to (31):

$$\Sigma_{YY}(s) = \frac{\beta^2}{2\alpha} (1 - e^{-2\alpha s}), \quad (31a)$$

$$\Sigma_{Y\tilde{V}}(s) = \Sigma_{\tilde{V}Y}(s) = \frac{\tilde{m}g\chi\beta^2}{\alpha - \gamma} \left[\frac{1 - e^{-(\alpha+\gamma)s}}{\alpha + \gamma} - \frac{1 - e^{-2\alpha s}}{2\alpha} \right], \quad (31b)$$

$$\begin{aligned} \Sigma_{\tilde{V}\tilde{V}}(s) &= \frac{\eta^2}{2\gamma} (1 - e^{-2\gamma s}) + \left(\frac{\tilde{m}g\chi\beta}{\alpha - \gamma} \right)^2 \\ &\times \left[\frac{1 - e^{-2\alpha s}}{2\alpha} + \frac{1 - e^{-2\gamma s}}{2\gamma} - 2 \frac{1 - e^{-(\alpha+\gamma)s}}{\alpha + \gamma} \right]. \end{aligned} \quad (31c)$$

It is essential to emphasize that, for the sake of notation, the expressions in (29b) and (31) refer to the matrix $\boldsymbol{\Sigma}(s)$ (which coincides with the covariance matrix conditioned to $\mathbf{X}(0) = \mathbf{x}_0$), whereas the covariance matrix of the Ornstein-Uhlenbeck process, shifted s_0 , reads more generally $\boldsymbol{\Sigma}(s - s_0)$.

Two important conclusions may be drawn. First, inspection of (29a) promptly reveals that the conditional expectation $\boldsymbol{\mu}(s | \mathbf{x}_0, s_0)$ solely depends on the deterministic component of the solution (27). Intuitively, this might be explained by recalling that the Ornstein-Uhlenbeck process (25) is Gaussian in nature, and observing that statistical variation around the mean is symmetrically distributed. Such a mathematical feature is a prerogative of the process, and similar arguments do not apply, in general, to the other physical quantities considered in the paper. The second consideration regards the existence of a stationary distribution for the Ornstein-Uhlenbeck process (25), which coincides with the limiting one obtained for $s_F, s \rightarrow \infty$, and is implied by the fact that the matrix $\mathbf{\Gamma}$ possesses eigenvalues $\lambda_1 = \alpha$ and $\lambda_2 = \gamma$ with a positive real part. The latter concept is also intimately related to the notion of ergodicity, which plays a crucial role in some considerations later drawn in Section IV. In particular, the concept of mean-ergodic processes is essential: a stochastic process whose ensemble average equals, in the limiting behavior, its time average. Analogous results may be derived by resorting to the alternative Fokker-Planck formalism, as detailed in the next Section III-B2.

2) *Fokker-Planck Equation*: The Fokker-Planck equation for the two-dimensional Ornstein-Uhlenbeck process (24) may be deduced starting directly with the general formula in (11), yielding the PDE of diffusion (32), shown at the bottom of the next page. As already anticipated in Section III-B1, the solution to the above PDE (32), equipped with a similar IC as in (13), is given by a bivariate normal PDF [55], [87], reading specifically as in (33), shown at the bottom of the next page, where the conditional mean $\boldsymbol{\mu}(s | \mathbf{x}_0, s_0)$ and the covariance matrix $\boldsymbol{\Sigma}(s)$ are as in (29). According to the above (33), $\mathbf{X}(s)$, conditional

to $\mathbf{X}(s_0) = \mathbf{x}_0$, follows a bivariate normal distribution, i.e.,

$$\mathbf{X}(s) | \mathbf{X}(s_0) = \mathbf{x}_0 \sim \mathcal{N}(\boldsymbol{\mu}(s | \mathbf{x}_0, s_0), \boldsymbol{\Sigma}(s - s_0)), \quad (34)$$

which is a property notoriously associated with diffusion-type PDEs. A complete derivation of (33), omitted in this paper for the sake of brevity, is detailed [55], [87]. In the context of the present work, it is instead interesting to observe that, coherently to what discussed already in the previous Section III-B, in the limits $s_F, s \rightarrow \infty$, the PDF (33) reduces to the stationary distribution

$$p(\mathbf{x}) = \frac{1}{\sqrt{|2\pi\boldsymbol{\Omega}|}} \exp\left(-\frac{1}{2}(\mathbf{x} - \boldsymbol{\theta})^T \boldsymbol{\Omega}^{-1}(\mathbf{x} - \boldsymbol{\theta})\right), \quad (35)$$

where $\boldsymbol{\theta} \equiv \mathbb{E}(\mathbf{X}(\infty))$, and $\boldsymbol{\Omega} \equiv \text{Cov}(\mathbf{X}(\infty), \mathbf{X}(\infty))$ satisfies the Lyapunov equation $\boldsymbol{\theta}\boldsymbol{\Omega} + \boldsymbol{\Omega}\boldsymbol{\theta}^T = \boldsymbol{\omega}\boldsymbol{\omega}^T$ [55]. Hence, in the limit case, (34) may be rewritten more conveniently as $\mathbf{X}(\infty) \sim \mathcal{N}(\boldsymbol{\theta}, \boldsymbol{\Omega})$, being the distribution independent of both the traveled distance and the IC. Clearly, the matrix $\boldsymbol{\Omega}$ may be deduced directly from the limiting expression $\boldsymbol{\Sigma}(\infty)$ for the time-dependent covariance matrix $\boldsymbol{\Sigma}(s)$, which corresponds to

$$\begin{aligned} \boldsymbol{\Omega} &= \begin{bmatrix} \Omega_{YY} & \Omega_{Y\tilde{V}} \\ \Omega_{\tilde{V}Y} & \Omega_{\tilde{V}\tilde{V}} \end{bmatrix} \\ &= \begin{bmatrix} \sigma_Y^2(\infty) & \rho_{Y\tilde{V}}\sigma_Y(\infty)\sigma_{\tilde{V}}(\infty) \\ \rho_{Y\tilde{V}}\sigma_Y(\infty)\sigma_{\tilde{V}}(\infty) & \sigma_{\tilde{V}}^2(\infty) \end{bmatrix}, \end{aligned} \quad (36)$$

where $\sigma_Y^2(\infty)$ and $\sigma_{\tilde{V}}^2(\infty)$ denote the stationary variances of the two processes, and $\rho_{Y\tilde{V}}$ their correlation coefficient. In particular, the following analytical expressions may be inferred for the entries of the matrix $\boldsymbol{\Omega}$ in (36):

$$\sigma_Y^2(\infty) = \frac{\beta^2}{2\alpha}, \quad (37a)$$

$$\sigma_{\tilde{V}}^2(\infty) = \frac{(\tilde{m}g\chi\beta)^2}{2\alpha\gamma(\alpha + \gamma)} + \frac{\eta^2}{2\gamma}, \quad (37b)$$

$$\rho_{Y\tilde{V}} = 2\tilde{m}g\chi\alpha\beta\sqrt{\frac{\gamma(\alpha + \gamma)}{\tilde{m}g\chi\beta + \eta\gamma(\alpha + \gamma)}}. \quad (37c)$$

Concluding the discussion about the Fokker-Planck formalism, it is perhaps beneficial to comment more extensively on the stationary, asymptotic, and ergodic behaviors of the Ornstein-Uhlenbeck process (25). First, as already mentioned, the limiting

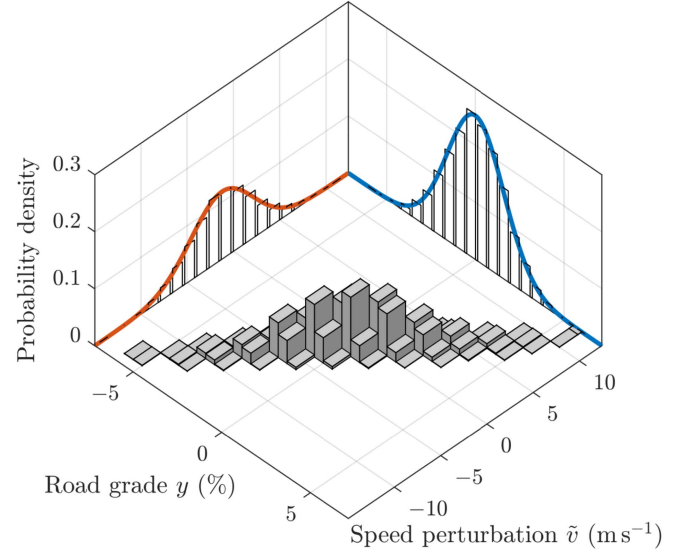


Fig. 4. Stationary bivariate normal distribution (35) for the Ornstein-Uhlenbeck process described by (25). The limiting mean and covariance matrix, appearing also in the stationary distribution, are given by $\boldsymbol{\theta}$ and $\boldsymbol{\Omega}$ as in (36). Model parameters: $\alpha = 9.16 \cdot 10^{-5} \text{ m}^{-1}$, $\beta = 0.021 \text{ m}^{-1/2}$, $\gamma = 0.0032 \text{ m}^{-1}$, $\tilde{m} = 0.045 \text{ s m}^{-1}$, $\theta_{\tilde{V}} = -1.236 \text{ m s}^{-1}$, $\eta = 1.85 \cdot 10^{-7} \text{ m}^3 \text{ s}^{-2}$.

PDF, given by (35), coincides with the stationary distribution. Essentially, this means that, for any IC of the type (13), the distribution of the process will approach the stationary one in the limits $s_F, s \rightarrow \infty$, losing therefore its memory about the original IC. Moreover, the PDF of an Ornstein-Uhlenbeck process starting with an initial distribution given according to (35) will not depend on time. Expanding upon the discussion initiated in Section III-B, it is worth remarking that the stationarity of the Ornstein-Uhlenbeck process (25) is a strict consequence of the fact the matrix $\boldsymbol{\Gamma}$ appearing in (25) has positive real eigenvalues, already calculated as $\lambda_1 = \alpha$ and $\lambda_2 = \gamma$.

Finally, Fig. 4 illustrates the stationary distribution of the Ornstein-Uhlenbeck process (25) generated numerically, along with the marginals and their analytical PDFs deduced from (35).

C. Propulsive Force, Power and Energy Consumption

The statistical properties of the main performance indicators needed for optimal vehicle design and control may be

$$\begin{aligned} \frac{\partial p(\mathbf{x}, s)}{\partial s} &= \frac{\partial}{\partial \tilde{v}} \left[\left(\gamma \tilde{v} - \tilde{m}g\chi y + f_r \tilde{m}g + \frac{1}{2} \rho_{\text{air}} C_d \tilde{A}_f v^* \right) p(\mathbf{x}, s) \right] \\ &+ \alpha \frac{\partial}{\partial y} [y p(\mathbf{x}, s)] + \frac{\eta^2}{2} \frac{\partial^2 p(\mathbf{x}, s)}{\partial \tilde{v}^2} + \frac{\beta^2}{2} \frac{\partial^2 p(\mathbf{x}, s)}{\partial y^2}, \quad (\mathbf{x}, s) \in \mathbb{R}^2 \times (s_0, s_F). \end{aligned} \quad (32)$$

$$\begin{aligned} p(\mathbf{x}, s | \mathbf{x}_0, s_0) &= \frac{1}{\sqrt{|2\pi\boldsymbol{\Sigma}(s - s_0)|}} \exp \left(-\frac{1}{2} (\mathbf{x} - \boldsymbol{\mu}(s | \mathbf{x}_0, s_0))^T \boldsymbol{\Sigma}^{-1} (s - s_0) (\mathbf{x} - \boldsymbol{\mu}(s | \mathbf{x}_0, s_0)) \right), \\ (\mathbf{x}, s) &\in \mathbb{R}^2 \times [s_0, s_F], \end{aligned} \quad (33)$$

inferred from the SDEs governing the longitudinal vehicle dynamics. More concretely, the knowledge of the distribution of the propulsive power delivered to the wheels, and the mean energy consumption constitute vital information when it comes to applying both offline and online optimization routines. The first quantity, in particular, requires the determination of the stochastic propulsive force. To this end, starting with (16) and (20), and neglecting the terms relating to the added white noise for simplicity, the following relationship may be deduced to approximately hold:

$$\tilde{F}_x(\mathbf{X}(s), s) \approx \mathbf{A}_k \mathbf{X}(s) + b_k, \quad (38)$$

where $\mathbf{A}_k \triangleq \mathbf{A}_{kp} + \mathbf{A}_{kd}$, and

$$\mathbf{A}_{kp} = -k_p \begin{bmatrix} 0 & 1 \end{bmatrix}, \quad (39a)$$

$$\mathbf{A}_{kd} = -v^* k_D \begin{bmatrix} \tilde{m} g \chi & -\gamma \end{bmatrix}, \quad (39b)$$

$$b_k = -v^* k_D \gamma \theta_{\tilde{V}} = v^* k_D \left(f_r \tilde{m} g + \frac{1}{2} \rho_{\text{air}} C_d \tilde{A}_f v^* \right). \quad (39c)$$

Together, (33) and (38) imply that the stochastic force follows a univariate normal distribution on $[s_0, s_F]$. With simplified notation compared to (38),

$$\tilde{F}_x(s) \mid \mathbf{X}(s_0) = \mathbf{x}_0 \sim \mathcal{N}(\mu_{\tilde{F}_x}(s \mid \mathbf{x}_0, s_0), \sigma_{\tilde{F}_x}^2(s - s_0)), \quad (40)$$

with mean and variance reading specifically

$$\begin{aligned} \mu_{\tilde{F}_x}(s \mid \mathbf{x}_0, s_0) &= \mathbb{E}(\tilde{F}_x(s) \mid \mathbf{X}(s_0) = \mathbf{x}_0) \\ &= \mathbf{A}_k \boldsymbol{\mu}(s \mid \mathbf{x}_0, s_0) + b_k, \end{aligned} \quad (41a)$$

$$\sigma_{\tilde{F}_x}^2(s) = \mathbb{V}\text{ar}(\tilde{F}_x(s)) = \mathbf{A}_k \boldsymbol{\Sigma}(s) \mathbf{A}_k^T. \quad (41b)$$

In the limit $s \rightarrow \infty$, the above mean and variance converge to the stationary values $\mu_{\tilde{F}_x}(\infty \mid \mathbf{x}_0, s_0) = \theta_{\tilde{F}_x} \equiv \mathbb{E}(\tilde{F}_x(\infty)) = \mathbf{A}_k \boldsymbol{\theta} + b_k$, and $\sigma_{\tilde{F}_x}^2(\infty) = \Omega_{\tilde{F}_x} \equiv \mathbb{V}\text{ar}(\tilde{F}_x(\infty)) = \mathbf{A}_k \boldsymbol{\Omega} \mathbf{A}_k^T$, therefore implying $\tilde{F}_x(\infty) \sim \mathcal{N}(\theta_{\tilde{F}_x}, \Omega_{\tilde{F}_x})$.

Accordingly, starting with (17), it might be inferred that the power $\tilde{P}_d(s)$, conditional to the IC, follows a censored normal distribution. In particular, its CDF may be written as

$$\begin{aligned} F_{\tilde{P}_d(s) \mid \mathbf{X}(s_0)}(P_d, s \mid \mathbf{x}_0, s_0) &= \mathbb{P}(\tilde{P}_d(s) \leq P_d \mid \mathbf{X}(s_0) = \mathbf{x}_0) \\ &= \Phi\left(\frac{P_d - v^* \mu_{\tilde{F}_x}(s \mid \mathbf{x}_0, s_0)}{v^* \sigma_{\tilde{F}_x}(s - s_0)}\right) \mathbb{1}_{P_d \in \mathbb{R}_{\geq 0}}, \end{aligned} \quad (42)$$

on $[s_0, s_F]$. The conditional expectation and variance may hence be deduced to be according to formulae (43), shown at the bottom of the page, where $\varphi(\cdot)$ and $\Phi(\cdot)$ denote the PDF and CDF of the standard normal distribution, respectively. Again, the mean and variance in the above (43) approach asymptotically the limiting values $\mu_{\tilde{P}_d}(\infty \mid \mathbf{x}_0, s_0) = \theta_{\tilde{P}_d} \equiv \mathbb{E}(\tilde{P}_d(\infty))$ and $\sigma_{\tilde{P}_d}^2(\infty \mid \mathbf{x}_0, s_0) = \Omega_{\tilde{P}_d} \equiv \mathbb{V}\text{ar}(\tilde{P}_d(\infty))$, whose analytical expressions are independent of the prescribed IC and may be easily deduced by combining (43) with (26) and (36).

It is also worth stressing that, as opposed to the expectation of the Ornstein-Uhlenbeck process, which was completely characterized by the deterministic part of (27), even the computation of the mean propulsive power, according to (43a), shown at the bottom of this page, presumes the knowledge of the covariance matrix $\boldsymbol{\Sigma}(s)$. An immediate implication is that the stochastic component of the SDE system (25) may play a crucial role in determining the energy performance of road vehicles. This is different from what was observed for the other quantities, whose mean only depended on the deterministic part of the SDEs (25). Mathematically, this phenomenon is dictated by the fact that the propulsive power delivered to the wheels behaves in a non-Gaussian way due to the truncation performed in (17) (energy harvesting is disregarded). However, the Gaussian behavior is approximately recovered for very large values of the expectation of the propulsive force (relatively to its standard deviation). The limiting CDF of the propulsive power, determined numerically from simulations, is depicted in Fig. 5, where a comparison is also shown with the analytical expression derived according to (42). Note that, in

$$\mu_{\tilde{P}_d}(s \mid \mathbf{x}_0, s_0) = \mathbb{E}(\tilde{P}_d(s) \mid \mathbf{X}(s_0) = \mathbf{x}_0) = v^* \mu_{\tilde{F}_x}(s \mid \mathbf{x}_0, s_0) \Phi\left(\frac{\mu_{\tilde{F}_x}(s \mid \mathbf{x}_0, s_0)}{\sigma_{\tilde{F}_x}(s - s_0)}\right) + v^* \sigma_{\tilde{F}_x}(s - s_0) \varphi\left(\frac{\mu_{\tilde{F}_x}(s \mid \mathbf{x}_0, s_0)}{\sigma_{\tilde{F}_x}(s - s_0)}\right), \quad (43a)$$

$$\begin{aligned} \sigma_{\tilde{P}_d}^2(s \mid \mathbf{x}_0, s_0) &= \mathbb{V}\text{ar}(\tilde{P}_d(s) \mid \mathbf{X}(s_0) = \mathbf{x}_0) = v^{*2} \mu_{\tilde{F}_x}^2(s \mid \mathbf{x}_0, s_0) \Phi\left(\frac{\mu_{\tilde{F}_x}(s \mid \mathbf{x}_0, s_0)}{\sigma_{\tilde{F}_x}(s - s_0)}\right) \left[1 - \Phi\left(\frac{\mu_{\tilde{F}_x}(s \mid \mathbf{x}_0, s_0)}{\sigma_{\tilde{F}_x}(s - s_0)}\right)\right] \\ &\quad + v^{*2} \mu_{\tilde{F}_x}(s \mid \mathbf{x}_0, s_0) \sigma_{\tilde{F}_x}(s - s_0) \varphi\left(\frac{\mu_{\tilde{F}_x}(s \mid \mathbf{x}_0, s_0)}{\sigma_{\tilde{F}_x}(s - s_0)}\right) \left[1 - 2\Phi\left(\frac{\mu_{\tilde{F}_x}(s \mid \mathbf{x}_0, s_0)}{\sigma_{\tilde{F}_x}(s - s_0)}\right)\right] \\ &\quad + v^{*2} \sigma_{\tilde{F}_x}^2(s - s_0) \left[\Phi\left(\frac{\mu_{\tilde{F}_x}(s \mid \mathbf{x}_0, s_0)}{\sigma_{\tilde{F}_x}(s - s_0)}\right) - \varphi^2\left(\frac{\mu_{\tilde{F}_x}(s \mid \mathbf{x}_0, s_0)}{\sigma_{\tilde{F}_x}(s - s_0)}\right)\right], \end{aligned} \quad (43b)$$

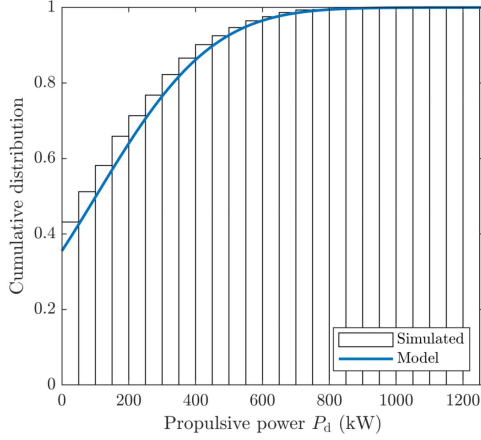


Fig. 5. Cumulative distribution of the stochastic propulsive power \tilde{P}_d , for a traveled distance of $s = 250$ km. According to (42), the propulsive power follows a censored normal distribution, with mean and variance given as in (43). Model parameters as in Fig. 4, with $v^* = 80 \text{ km h}^{-1}$, $k_p = 3583 \text{ N s m}^{-1}$, and $k_D = 0 \text{ N s}^2 \text{ m}^{-1}$.

Fig. 5, the realizations of the propulsive power are denoted by P_d .

Finally, the total energy required to travel a distance equal to $\Delta s = s_F - s_0$, and the corresponding energy consumption, may be calculated with the aid of (18) and (19), and their moments determined numerically. In particular, concerning the energy consumption, it is also worth observing that, since the noise term has been neglected in (38), the continuity of the paths of the Ornstein-Uhlenbeck process $\{\mathbf{X}(s)\}_{s \in [s_0, s_F]}$ implies that also $\{\tilde{F}_x(s)\}_{s \in [s_0, s_F]}$ and $\{\tilde{P}_d(s)\}_{s \in [s_0, s_F]}$ have continuous paths. Concerning the calculation of the mean value $\mu_{\tilde{e}_d}(s_F | \mathbf{x}_0, s_0)$ of the energy consumption $\tilde{e}_d(s_F)$ over the traveled distance s_F per distance unit, an application of Fubini's theorem (see, e.g., Theorems 2.39 and 8.40 in [70] or Theorem 2.39 in [88]) yields consequently

$$\begin{aligned} \mu_{\tilde{e}_d}(s_F | \mathbf{x}_0, s_0) &= \mathbb{E}(\tilde{e}_d(s_F) | \mathbf{X}(s_0) = \mathbf{x}_0) \\ &\approx \frac{1}{v^*(s_F - s_0)} \mathbb{E}\left(\int_{s_0}^{s_F} \tilde{P}_d(s) ds \mid \mathbf{X}(s_0) = \mathbf{x}_0\right) \\ &= \frac{1}{v^*(s_F - s_0)} \int_{s_0}^{s_F} \mathbb{E}(\tilde{P}_d(s) | \mathbf{X}(s_0) = \mathbf{x}_0) ds \\ &= \frac{1}{v^*(s_F - s_0)} \int_{s_0}^{s_F} \mu_{\tilde{P}_d}(s | \mathbf{x}_0, s_0) ds, \end{aligned} \quad (44)$$

whose integrand is known analytically from (43a) (note that the integral in (44) still needs to be evaluated numerically). The above formula (44) for the mean energy consumption is valid for any values of the traveled distance s_F , and presumably dependent on it. However, for very large values of s_F , and in particular in the limit $s_F \rightarrow \infty$, the following pragmatic approximation appears reasonable:

$$\begin{aligned} \mu_{\tilde{e}_d}(s_F | \mathbf{x}_0, s_0) &\approx \theta_{\tilde{e}_d} = \mu_{\tilde{e}_d}(\infty | \mathbf{x}_0, s_0) \\ &\approx \frac{\mu_{\tilde{P}_d}(\infty | \mathbf{x}_0, s_0)}{v^*} = \frac{\theta_{\tilde{P}_d}}{v^*}, \end{aligned} \quad (45)$$

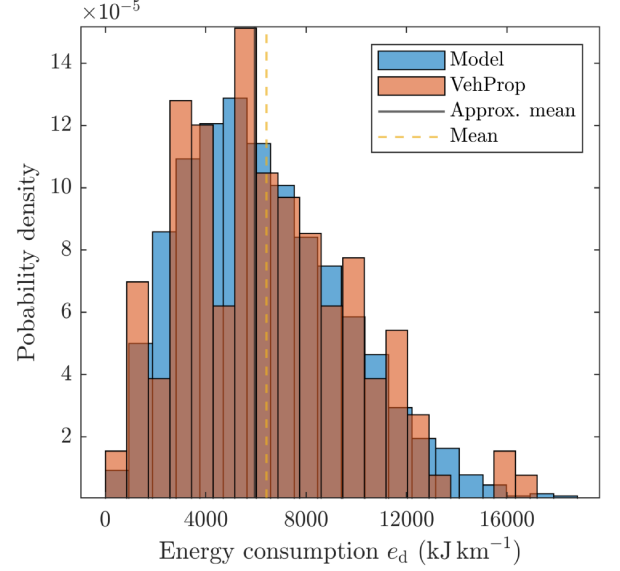


Fig. 6. Distribution of the stochastic energy consumption \tilde{e}_d according to the model prediction (3000 sample paths), and 300 simulations in VehProp, for a total traveled distance of $\Delta s = s_F - s_0 = 50$ km. The expectations appearing are the exact one (dashed yellow line), computed numerically and amounting to $6.42 \cdot 10^3 \text{ kJ km}^{-1}$, and the corresponding approximation obtained using (45) (gray line), amounting to $5.95 \cdot 10^3 \text{ kJ km}^{-1}$ (relative error of 7.32%). Model parameters as in Figs. 4 and 5.

which is also legitimated by the ergodic and stationary behavior of the Ornstein-Uhlenbeck process (25) (it is worth recalling, in this context, that the energy consumption in (44) is proportional to the time average of the stochastic power). The analytical expression deduced according to (45) is, of course, exact (for any value of s_F) for any IC of the type (35), for which the Ornstein-Uhlenbeck (25) process is strictly stationary. This observation is propaedeutic to the building of the ergodic theory of energy consumption undertaken in the next Section IV.

At conclusion of this one, instead, Fig. 6 compares the PDF of the energy consumption¹⁰ generated numerically with some results obtained in VehProp, a higher-fidelity simulation model for investigations concerned with longitudinal vehicle dynamics [50], [67]. More specifically, VehProp allows the modeling of the operating environment using discrete-time stochastic processes, as opposed to the continuous formulations proposed in this paper. Combined with more sophisticated equations for the longitudinal motion of road vehicles, including also nonlinear effects neglected in (24b), this enables the accurate estimation of vehicular performance like, for instance, energy consumption. In particular, the topography parameter was generated in VehProp using the equivalent AR(1) representation of the Ornstein-Uhlenbeck process (23) [50], [67]. The agreement between model prediction and simulations in VehProp is encouraging. In Fig. 6, the comparison between the expectations calculated according to (44) and (45) is also shown, which appears to confirm the validity of the approximation (45). The mean value of the data generated with VehProp is not reported in Fig. 6, since

¹⁰As for the propulsive power, the realizations of the energy consumption are denoted by e_d , i.e., using the corresponding letter without the tilde.

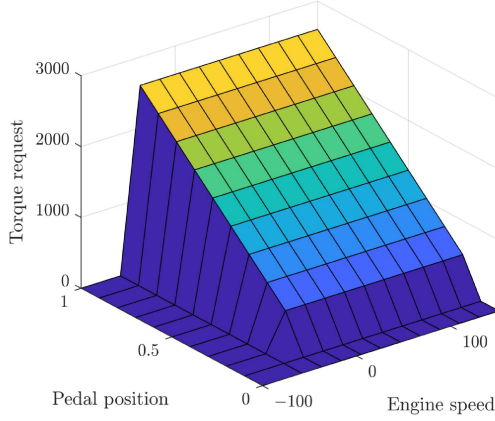


Fig. 7. Torque request map as a function of the acceleration pedal position and engine's speed.

it was indistinguishable from the exact one computed according to (44).

IV. AN ERGODIC THEORY OF ENERGY CONSUMPTION

Except for some mathematical simplifications introduced to facilitate the calculations, the theory exemplified in Section III, restricted to homogeneous road sections, may be fairly considered to be exact. The present analysis is instead devoted to the development of an approximated statistical theory to predict the energy consumption of road vehicles. Continuing the discussion commenced in the introductory part of the manuscript, such a theory should be regarded as an ergodic one, meaning that it presumes that the stochastic processes governing the longitudinal vehicle dynamics are ergodic, and admit stationary distributions on each homogeneous segment with conditional parameters ξ_i^* . The ergodicity over the long and thus non-homogeneous segments is achieved through assumptions that there is some overall statistical distribution of the parameters that accounts for non-homogeneity and that homogeneous and stationary segments are sampled independently from this distribution. This setting is in line with the assumption that energy consumption results from many independent journeys undertaken by a vehicle within the homogeneous conditions. The theory outlined in the following is approximated, in the sense that it deliberately disregards transient dynamics connected with the transitions between different road segments.

The next Section IV-A presents the main ideas and formalisms on which the treatment is grounded, whereas Section (IV-B) is devoted to the numerical corroboration of the proposed theory, whose predictions are again validated against simulation results obtained in VehProp. In particular, an example is adduced where the stochastic road models and vehicle's parameters are supposed to depend on the legal speed.

A. Conditional Distributions and Moments on Homogeneous Road Sections

The intent of the present section is that of deducing the salient statistical properties of the main physical quantities in interest,

concerning entire road missions or transport applications. To this end, the considered vehicle is supposed to travel extremely long distances (i.e., the limits $s, s_F \rightarrow \infty$ are considered), so that the PDF, CDF, and moments of the speed fluctuations, propulsive power, and energy consumption may be inferred from the limiting, or stationary ones already computed in Section III, by applying the total laws for probability, expectation, and variance. Concretely, this mathematical assumption translates into the hypothesis that the actual sequence of homogeneous road segments traveled by the vehicle does not influence its energy performance. This is approximately satisfied if, as conveniently supposed, infinitely long transport missions are considered. In this case, all the relevant physical quantities become independent of the traveled distance, and the laws of total probability, expectation, and variance yield a weighted summation, where the weighting coefficients (or probabilities) represent the stationary distribution of each homogeneous road segment, sampled independently according to some fixed law. In this way, mixture models for the quantities in interest may be deduced from their conditional formulations. To proceed with the analysis, it is also essential to remark that all the equations and quantities considered in Section III, where the dependence upon the set of parameters ξ^* had been omitted for readability, should be henceforth interpreted as conditional. Furthermore, and merely for simplicity, it will be assumed that the variables Ξ^* only take values in a discrete sample space, i.e., $\Xi^* = \xi_i^*, i \in \{1, \dots, r\}$, with probability mass function π_i corresponding to a stationary or limiting distribution, as already anticipated. For instance, the corresponding SDE system of (25), conditional to $\Xi^* = \xi_i^*$, would then become

$$d\mathbf{X}(s) = \mathbf{\Gamma}(\xi_i^*)(\boldsymbol{\theta}(\xi_i^*) - \mathbf{X}(s))ds + \boldsymbol{\omega}(\xi_i^*)d\mathbf{B}_{\mathbf{X}}(s), \quad s \in (s_0, s_F), \quad (46)$$

where now the dependence upon the set of parameters ξ_i^* has been explicitly highlighted. From the above SDE-based description, an analogous Fokker-Planck PDE to (32) could be derived, with stationary solution given by the conditional PDF

$$p(\mathbf{x} \mid \xi_i^*) = \frac{1}{\sqrt{2\pi\boldsymbol{\Omega}(\xi_i^*)}} \times \exp\left(-\frac{1}{2}(\mathbf{x} - \boldsymbol{\theta}(\xi_i^*))^T \boldsymbol{\Omega}^{-1}(\xi_i^*)(\mathbf{x} - \boldsymbol{\theta}(\xi_i^*))\right), \quad (47)$$

where $\boldsymbol{\theta}(\xi_i^*)$ and $\boldsymbol{\Omega}(\xi_i^*)$ denote the stationary mean and covariance matrix, interpreted as conditional to the realization ξ_i^* of the random variables Ξ^* .

The stationary distribution of $\mathbf{X}(s)$ obtained by stochastically mixing the parameter Ξ^* of the Ornstein-Uhlenbeck processes is thus given by the density

$$f_{\mathbf{X}}(\mathbf{x}) = \sum_{i=1}^r p(\mathbf{x} \mid \xi_i^*) \mathbb{P}(\Xi^* = \xi_i^*) = \sum_{i=1}^r p(\mathbf{x} \mid \xi_i^*) \pi_i. \quad (48)$$

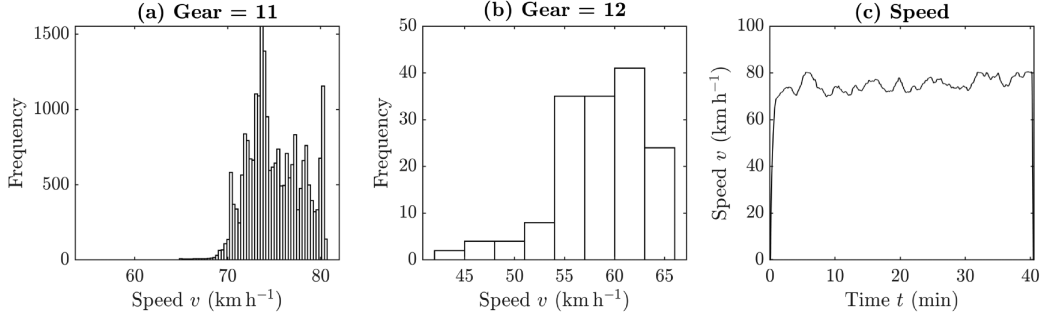


Fig. 8. Frequency of the two main gear ratios on a road segment with legal speed of $v_i^* = 80 \text{ km h}^{-1}$ (Fig. 8(a) and (b), respectively), and corresponding dynamic speed profile (Fig. 8(c)), obtained from a simulation in VehProp (total traveled distance $s_F = 50 \text{ km}$).

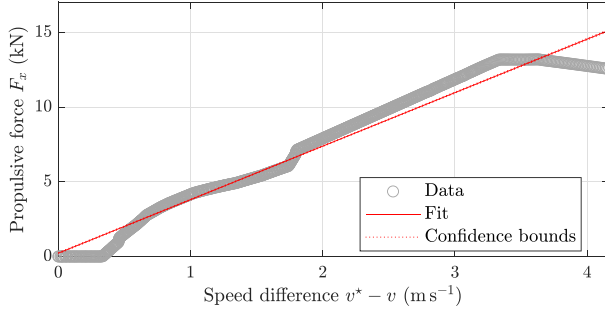


Fig. 9. Value of the proportional gain $k_{P,i}$ for a highway section with reference speed $v_i^* = 80 \text{ km h}^{-1}$, fitted from simulation data generated in VehProp (total traveled distance $s_F = 50 \text{ km}$).

Recalling the formulae previously derived in Section III-B2, perfectly analogous calculations would yield the analytical expressions for the total expectation and variance. This would yield a mixture model for the road grade and vehicle's speed. Similarly, the total stationary CDF of the stochastic propulsive power, its mean and variance, may also be determined following the same rationale.

In what follows, the focus is predominantly on the energy consumption, which, based on the stationary formula (45), may thus be deduced to be

$$\begin{aligned} \mathbb{E}(\tilde{e}_d(\infty)) &= \sum_{i=1}^r \mathbb{E}(\tilde{e}_d(\infty) \mid \Xi^* = \xi_i^*) \mathbb{P}(\Xi^* = \xi_i^*) \\ &= \sum_{i=1}^r \theta_{\tilde{e}_d}(\xi_i^*) \pi_i = \sum_{i=1}^r \frac{\theta_{\tilde{P}_d}(\xi_i^*)}{v_i^*} \pi_i = \theta_{\tilde{e}_d}, \end{aligned} \quad (49)$$

where the last equation serves as the definition of $\theta_{\tilde{e}_d}$ and should not be confounded with the expectation appearing in (45), now regarded as conditional on the parameters.

B. An Example With Road Types and Legal Speed

To validate the ergodic theory developed above, the energy consumption predicted according to (49) is again compared to simulation results obtained in VehProp. As opposed

to the example adduced in Section III-C, the following analysis is concerned with an entire population of complete road transport missions, accounting for transitions between homogeneous road segments. In turn, these are classified depending on the specific combination of road type and legal speed.

The next Section IV-B1 explains in great detail the procedure followed to parametrize the stochastic model for longitudinal vehicle dynamics, whereas Section IV-B2 is dedicated to the comparison with numerical simulations.

1) *Model Construction and Parametrization:* The operating cycle considered in the following coincides to that parametrized in [48], Table 7), and is representative of the usage of heavy-duty vehicles traveling long distances in the region of Västra Götaland, Sweden. In the context of the present paper, it is however essential to clarify that not all the parameters listed in [48] have been included in the modeling of the operating environment, which has instead been restricted to three main characteristics, namely, road type, legal speed, and topography. The values for the corresponding model parameters, v_i^* , α_i , and β_i , $i \in \{1, \dots, 7\}$, are collected in Table I, where the first three values refer to urban road sections, those from four to six to rural segments, and the last one to highway portions of the road. The stationary distributions π_i associated with each combination of road type and legal speed are also listed in Table I, and have been deduced in a previous work directly from measurement data collected from 33 different trucks [48]. Concerning instead the stochastic modeling of the operating environment, the adopted procedure is standard: first, the sequence of road types is generated using an ergodic, continuous-time Markov chain [47], [48]; then, the sequences of legal speeds and topography, conditional to each road type, are simulated respectively using another continuous-time Markov chain [47], [48], and the AR(1) process equivalent to the Ornstein-Uhlenbeck formulation (23) proposed in this work, with parameters α_i and β_i given as in Table I. In particular, the parameters of the Ornstein-Uhlenbeck process (23) may be observed to exclusively depend on the road type, whereas the legal speed values are not influential in their determination. For an interested reader, exhaustive details on how to synthesize virtual operating environments in VehProp are reported, e.g., in [50], [67].

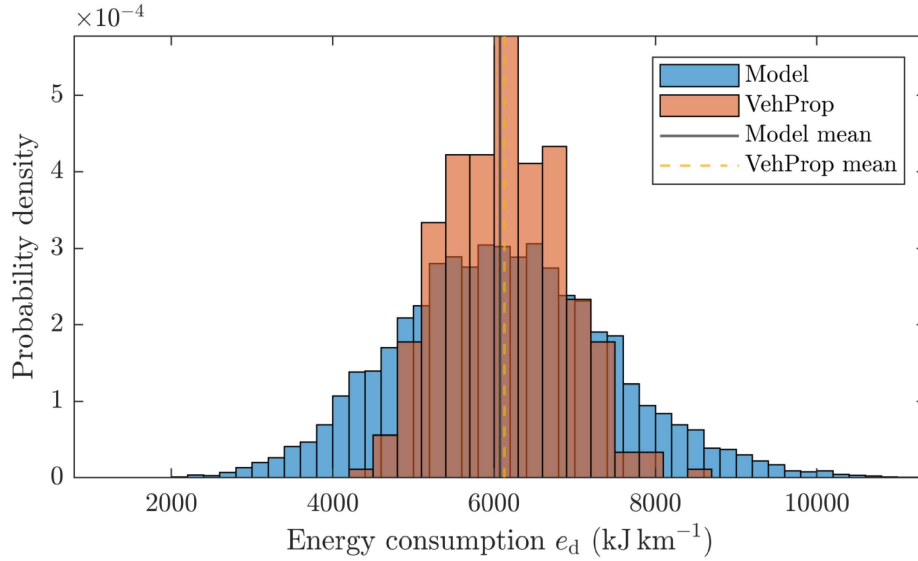


Fig. 10. Distribution of the stochastic energy consumption \tilde{e}_d according to the model prediction (10000 sample paths, with proportions given by the stationary distributions π_i , $i \in \{1, \dots, 7\}$, reading as in Table I), and 300 simulations in VehProp, for a total traveled distance of 500 km. The expectations appearing are the numerical one from VehProp (dashed yellow line), amounting to $6.13 \cdot 10^6$ kJ km $^{-1}$, and the analytical one deduced according to (45) (gray line), amounting to $6.07 \cdot 10^3$ kJ km $^{-1}$ (relative error of 0.98%). Model parameters as in Table I.

TABLE I
MODEL PARAMETERS FOR EACH COMBINATION OF ROAD TYPE AND LEGAL SPEED

Realization i		1	2	3	4	5	6	7
Probability π_i		0.0151	0.0146	0.0429	0.0381	0.1022	0.4474	0.3396
Road type		Urban			Rural			Highway
Quantity	Unit				Value			
v_i^*	km h ^{−1}	30	40	50	60	70	80	80
α_i	m ^{−1}	$5.93 \cdot 10^{-4}$	$5.93 \cdot 10^{-4}$	$5.93 \cdot 10^{-4}$	$7.61 \cdot 10^{-5}$	$7.61 \cdot 10^{-5}$	$7.61 \cdot 10^{-5}$	$9.16 \cdot 10^{-5}$
β_i	m ^{−1/2}	0.079	0.079	0.079	0.022	0.022	0.022	0.021
γ_i	m ^{−1}	0.031	0.018	0.009	0.0064	0.0045	0.002	0.0031
\tilde{m}_i	s m ^{−1}	0.120	0.090	0.072	0.060	0.051	0.045	0.045
$\rho_{\text{air},i}$	kg m ^{−3}	1.225	1.225	1.225	1.225	1.225	1.225	1.225
$\tilde{A}_{f,i}$	m ² kg ^{−1}	$1.85 \cdot 10^{-4}$	$1.85 \cdot 10^{-4}$	$1.85 \cdot 10^{-4}$	$1.85 \cdot 10^{-4}$	$1.85 \cdot 10^{-4}$	$1.85 \cdot 10^{-4}$	$1.85 \cdot 10^{-4}$
η_i	m ³ s ^{−2}	0	0	0	0	0	0	0
$k_{\text{P},i}$	N s m ^{−1}	13763	10783	6892	5598	4576	2276	3583
$k_{\text{D},i}$	N s ² m ^{−1}	0	0	0	0	0	0	0

The other variables appearing in Table I refer instead to the vehicle's design attributes and driver's control action. According to the relationships deduced in (21), their values are subordinate to the choice of reference speed, which, by assumption, coincides with the legal speed v_i^* on each homogeneous road section. Specifically, the values listed in Table I are typical of a heavily-loaded Volvo FH13 rigid truck, equipped with a diesel engine and an actuated, stepped gearbox with 12 forward gears. Since in VehProp the operational driver's behavior is modeled as a PD controller concerning the pedal position rather than directly the speed difference¹¹, the proportional gains $k_{P,i}$, $i \in \{1, \dots, 7\}$,

need to be calculated starting with the static map for the torque request, shown for completeness in Fig. 7, and then reduced to the wheel level under the assumption of no-slip conditions (it should be observed that the torque request is fairly constant with the engine's speed). In this context, the $k_{P,i}$ terms also account implicitly for the gear ratio coefficient, which has been supposed for simplicity to be constant on each road segment, and solely dependent on the reference velocity v_i^* . Therefore, to correctly parametrize the stochastic model proposed in this paper, the predominant gear ratio has been determined numerically for each combination of road type and legal speed, and the gain $k_{P,i}$ has been computed accordingly. For instance, Fig. 8(a) and (b) illustrate the frequency of the two main gears selected on a highway segment, along with the corresponding dynamic speed profile (Fig. 8(c)), for a maximum allowed limit of 80 km h $^{-1}$ and a total length of $s_F = 50$ km. The result of the fitting

¹¹As previously mentioned, the driver model in VehProp is composed of several modules, separated into tactical and operational parts. The vehicle model is also quite sophisticated and includes submodules for powertrain and chassis dynamics.

procedure, repeated for each of the cases listed in Table I, is instead depicted in Fig. 9 considering the 11th gear. On the other hand, the derivative action has been deliberately disregarded to facilitate the analysis (i.e., $k_{D,i} = \eta_i = 0$), but its influence is usually negligible. Similarly, the term \tilde{m}_i has not been adjusted to incorporate the inertial contributions originating from the rotating elements, which, in the context of the present study, may be foreseen to have only a minor impact on the predicted energy consumption due to the extremely high values of the vehicle's mass.

2) *Simulation Results and Model Comparison:* A total of 300 operating cycles was simulated in VehProp using the longitudinal vehicle dynamics model detailed in [50], [67], considering stochastically generated environments according to the procedure outlined in Section IV-B1. For the present study, a total distance of 500 km was prescribed to ensure that the proportions of the different road segments synthesized using the double-Markov-chain-algorithm approached the stationary distributions $\pi_i, i \in \{1, \dots, 7\}$, listed in Table I. Moreover, this expedient allowed for mitigating the effect of transient dynamics excited by the transition between homogeneous road segments with different road characteristics. The value $\Delta s = s_F - s_0 = 500$ km should hence be thought of as indicative of infinitely long traveled distances $s_F \rightarrow \infty$. Simulating the entire population of operating cycles required a total of 7.6 hours, with an average simulation time of 1.52 min (the minimum and maximum for cycle being 1.21 and 2.41 min, respectively). Concerning instead the analytical formulation, 10000 sample paths were simulated using the novel SDE-based formulation, again with $\Delta s = s_F - s_0 = 500$ km and proportions coinciding with the stationary distributions reported in Table I. The time needed to simulate 10000 sample paths amounted approximately to 20.91 s, with a minimum and maximum simulation time of 0.33 and 9.54 s for the second sixth realizations in Table I. In this context, and regarding specifically the calculation of the mean energy consumption, it is also essential to remark that the equivalence between the proportions of sample paths and traveled distance is sanctioned by the ergodic properties enjoyed by the model.

Fig. 10 compares the PDF of the energy consumption predicted according to the analytical formulation (blue histogram), and simulations performed in VehProp (orange histogram). Albeit the two expectations – amounting respectively to $6.07 \cdot 10^3$ and $6.13 \cdot 10^3$ kJ km⁻¹ – practically coincide, with a relative error below 1%, the distribution predicted analytically exhibits longer tails. To explain such a discrepancy, numerical simulations have also been conducted using the nonlinear version of (24b), without observing any major difference with the distribution obtained using the simplified formulation. A better agreement between theoretical predictions and simulation results may be achieved in future studies by considering refined driver models, accounting for transient and dynamical effects that are not captured by the current implementation.

V. DISCUSSION AND CONCLUSION

The present section concludes the paper by recapitulating the main results and offering some directions for future research.

A. Discussion

This present work constitutes the first attempt at a complete stochastic approach to the modeling of longitudinal road vehicle motion. Specifically, the proposed theory combines SDEs of diffusion, describing the salient properties of the operating environment and vehicle dynamics, with an alternative PDE-based formalism (the corresponding Fokker-Planck equation), which allows deducing the statistical properties of the involved quantities either analytically or numerically. Inspired by classic results from fundamental disciplines like physics [56], chemistry [57], and contact mechanics [59], [60], the main intuition behind the formulation proposed in the paper resides in that the statistics of the main energy performance indicators of road vehicles – including, e.g., propulsive power delivered to the wheels and energy consumption – are intimately related to those of the physical variables that appear explicitly in the equations of motions. Hence, if their dynamics are known, at least in a statistical sense, the vehicle's motion may also be determined using the well-established methods of stochastic calculus. In fact, as opposed to previous studies dedicated to the synthesis of conventional representations or transport missions in the form of driving and operating cycles, the methodology introduced in this paper directly incorporates the stochastic component of the environmental factors into the governing equations of the model. As a consequence, there is no need to supplement the resulting description of the environment with additional models of the vehicle and driver.

The mathematical aspects of the theory presented in this paper, the specific choices of models, and their possible generalizations also deserve a proper discussion. First, it is worth remarking that, except for some analytical simplifications, when restricted to homogeneous road segments, the theory developed in Sections II and III is methodologically correct, and may fairly be regarded as exact. Therefore, building upon the conclusions drawn in Section III, it does not seem incautious to conjecture that it should always be capable of explaining the essential phenomena connected with stochasticity in speed fluctuations, instantaneous power requests, and consumed energy, independently of the specific stochastic processes employed to model the road and mission characteristics. On the other hand, the main examples adduced in the manuscript were concerned with relatively simple special cases of the general theory outlined in Section II, and confined to an Ornstein-Uhlenbeck process describing the road topography parameter and vehicle's speed perturbation. The mathematical properties of such a process and its associated Fokker-Planck equation – including the existence of stationary and limiting distributions – have been extensively studied in the literature and, in the context of the present works, have offered a fertile terrain for further reflections. More concretely, they have been propaedeutic to the subsequent analyses conducted in Section IV. Indeed, only under certain (reasonable) assumptions of ergodicity can the general theory of Sections II and III be extended, in an approximate way, to estimate the energy performance of road vehicles when considering entire transport missions and applications. In the present paper, this was achieved

by deriving mixture models for the quantities in interest, by combining their conditional formulations with the distributions of road types and legal speeds. However, estimating the energy consumption also represents the ultimate ambition of more conventional descriptions like driving and operating cycles, and therefore care should be taken when the different approaches are juxtaposed. For the same purpose, possible generalization to the models considered in Section III should desirably preserve the stationary and ergodic properties of the Ornstein-Uhlenbeck process.

Intimately related to these aspects, the notion of energy consumption itself is particularly delicate, and merits special attention. It seems natural to assume that such a scalar metric be independent of the traveled distance, which automatically supports the argument in favor of the existence of stationary and limiting distributions¹². Owing to such premises, identifying the energy consumption with the expectation of (19), computed in the limit $s_F \rightarrow \infty$, eventually appears to constitute an inescapable prerequisite for its rigorous mathematical conceptualization.

B. Conclusions and Outlook on Future Work

This paper introduced a novel theory of longitudinal road vehicle dynamics, where the stochastic variation due to environmental factors is considered directly in the governing equations of motion. Depending on the relevant characteristics of the operating environment, the proposed SDE-PDE formulation may enable rapid and accurate estimation of performance indicators like mean CO₂ emissions, state-of-charge, and energy consumption, as also partially corroborated numerically in Section IV. Moreover, by eliminating the need for simulating large populations of driving and operating cycles, it may be conveniently combined with standard algorithms and routines to support the development of energy-efficient vehicles at reduced computational costs. For instance, the closed-form expressions derived according to (43), (45), and (49) may be used directly as inputs to vehicle's design optimization problems, minimizing, e.g., the energy consumption or the total cost of ownership, and treating the propulsive power as a constraint. Optimal solutions obtained following this rationale may be then tested against dynamic models in simulations, or utilized as initial conditions to larger and more complex optimization problems [51]. Besides its potential applications, the statistical theory outlined in this paper describes how road vehicles move and consume building on sound first-order principles, and offers a full physical-analytical alternative to the commonly available empirical formulations [65], [66].

Several possible extensions could also be explored in the immediate future. First, concerning the road topography parameter, more advanced and realistic models than the Ornstein-Uhlenbeck process considered in Section III could be adopted [84], [85]. For example, previous research has suggested that Laplace models could more accurately capture the variation of the topography parameter over longer road segments [84], [85].

¹²Intuitively, the consumed energy should be calculated by simply multiplying the energy consumption by the traveled distance. For such an operation to be mathematically valid, the energy consumption would obviously need to be constant with the traveled distance.

Nonlinear effects connected with the presence of trigonometric functions in the more general (2) could also be investigated numerically (existence and uniqueness following immediately from the same theorems invoked in Section III-B1). Starting with the ergodic theory presented in Section IV, the influence of the road curvature on the energy performance may also be taken into account, in an approximated way, using the analytical formulae reported in [47], [48]. Indeed, curvy roads are likely to influence the driver choice of speed, which might not coincide with the legal one. Several different driver models, such as those presented in [74], [75], [76], [77], [78], may also be adapted to the proposed framework, in conjunction with longitudinal equations of motions, to provide a more realistic energy consumption estimation. Similarly, on homogeneous road segments, the effect of high traffic densities may be investigated using a fundamental diagram relationship dictating the driver's choice of speed. These extensions may require employing different fundamental diagrams and/or car-following models, depending on the specific road type considered (urban, rural, highway), but would not introduce any major modifications to the theory proposed in the paper. Advanced powertrain models, possibly considering transient dynamical effects and internal losses, could also be integrated within the proposed formulation; this would lead to a more reliable estimation of energy performance. Finally, it should be mentioned that some of the simplifications introduced in the paper, for instance, the linearization performed in (5), are not crucial to the development of the theory, and may be removed in future refinements, without affecting the main conclusions drawn in this work.

APPENDIX

The present appendix collects some additional results concerning a more general SDE system than that in (24), derived from the assumption that the driver behaves as a PID controller.

A. Ornstein-Uhlenbeck Topography Model With PID Driver Controller

Considering a more general PID driver model, in the time domain, the expression for the propulsive force should be modified as

$$\begin{aligned} F_x(v(t), \dot{v}(t), w(t), \zeta(t), t) = & k_P(v^* - v(t)) \\ & + k_I \int_{t_0}^t (v^* - v(t')) dt' \\ & + F_{x0} - k_D \dot{v}(t) + k_N w(t), \end{aligned} \quad (50)$$

where, in addition to the new integral term, the quantity F_{x0} appears to account for a possibly nonzero initial force. Including the latter is necessary, since, at the beginning of each road segment, the PID control action might have already accumulated an initial force produced by the integral term. To recover strong solutions to the resulting SDE system, it will henceforth be supposed that F_{x0} be independent of the σ -algebra generated by the corresponding Brownian motion $\{\mathbf{B}_X(s)\}_{s \in [s_0, s_F]}$, and additionally that $\mathbb{E}(|F_{x0}|^2) < \infty$ (where the absolute value $|\cdot|$ is a norm on a finite-dimensional space for a scalar variable). Owing to these technical assumptions, the presence of the integral

term may be appropriately handled by defining:

$$\tilde{x}(t) \triangleq \int_{t_0}^t \tilde{v}(t) - \frac{F_{x0}}{k_1}, \quad (51)$$

or equivalently, in differential form, $\dot{\tilde{x}}(t) = \tilde{v}(t)$, with IC reading $\tilde{x}_0 = \tilde{x}(0) = -F_{x0}/k_1$.

With a similar rationale as in Section III-B1, the governing SDEs of the longitudinal vehicle dynamics may be deduced as follows:

$$dY(s) = -\alpha Y(s)ds + \beta dB_Y(s), \quad (52a)$$

$$d\tilde{X}(s) = \frac{1}{v^*} \tilde{V}(s)ds, \quad (52b)$$

$$\begin{aligned} d\tilde{V}(s) = & -\left(\gamma \tilde{V}(s) + \psi \tilde{X}(s) - \tilde{m}g\chi Y(s)\right)ds \\ & -\left(f_r \tilde{m}g + \frac{1}{2}\rho_{\text{air}}C_d \tilde{A}_f v^*\right)ds \\ & + \eta dB_{\tilde{V}}(s), \quad s \in (s_0, s_F), \end{aligned} \quad (52c)$$

being γ , \tilde{m} , \tilde{A}_d , and η defined as in (21), and

$$\psi \triangleq \frac{k_1}{v^*(m^* + k_D)}. \quad (53)$$

Equations (52) may be restated in vector form as in (25), but with (26) replaced by

$$\mathbf{\Gamma} = \begin{bmatrix} \gamma_{YY} & \gamma_{Y\tilde{X}} & \gamma_{Y\tilde{V}} \\ \gamma_{\tilde{X}Y} & \gamma_{\tilde{X}\tilde{X}} & \gamma_{\tilde{X}\tilde{V}} \\ \gamma_{\tilde{V}Y} & \gamma_{\tilde{V}\tilde{X}} & \gamma_{\tilde{V}\tilde{V}} \end{bmatrix} \triangleq \begin{bmatrix} \alpha & 0 & 0 \\ 0 & 0 & -\frac{1}{v^*} \\ -\tilde{m}g\chi & \psi & \gamma \end{bmatrix}, \quad (54a)$$

$$\boldsymbol{\theta} = \begin{bmatrix} \theta_Y \\ \theta_{\tilde{X}} \\ \theta_{\tilde{V}} \end{bmatrix} \triangleq -\frac{1}{\gamma} \begin{bmatrix} 0 \\ 0 \\ f_r \tilde{m}g + \frac{1}{2}\rho_{\text{air}}C_d \tilde{A}_f v^* \end{bmatrix}, \quad (54b)$$

$$\boldsymbol{\omega} = \begin{bmatrix} \omega_{YY} & \omega_{Y\tilde{V}} \\ \omega_{\tilde{X}Y} & \omega_{\tilde{X}\tilde{V}} \\ \omega_{\tilde{V}Y} & \omega_{\tilde{V}\tilde{V}} \end{bmatrix} \triangleq \begin{bmatrix} \beta & 0 \\ 0 & 0 \\ 0 & \eta \end{bmatrix}. \quad (54c)$$

Using (52) and (54), the solution to the considered SDE system is formally equivalent to that reported in (27), but with a rather involved expression for the corresponding matrix exponential $e^{-\mathbf{\Gamma}s}$:

$$e^{-\mathbf{\Gamma}s} = \begin{bmatrix} \Gamma_1(s) & \Gamma_2(s) & \Gamma_3(s) \\ \Gamma_4(s) & \Gamma_5(s) & \Gamma_6(s) \\ \Gamma_7(s) & \Gamma_8(s) & \Gamma_9(s) \end{bmatrix}, \quad (55)$$

where

$$\Gamma_1(s) = e^{-\alpha s}, \quad (56a)$$

$$\Gamma_2(s) = \Gamma_3(s) = 0,$$

$$\begin{aligned} \Gamma_4(s) = & -\frac{\tilde{m}g\chi\varrho_4(\varrho_1(s) + \varrho_2(s) - 2\Gamma_1(s))}{\varrho_3} \\ & -\frac{\tilde{m}g\chi\sqrt{v^*}(2\alpha - \gamma)(\varrho_1(s) - \varrho_2(s))}{\varrho_3}, \end{aligned} \quad (56b)$$

$$\Gamma_5(s) = \frac{\varrho_4(\varrho_1(s) + \varrho_2(s)) - \gamma\sqrt{v^*}(\varrho_1(s) - \varrho_2(s))}{2\varrho_4}, \quad (56c)$$

$$\Gamma_6(s) = -\frac{\varrho_1(s) - \varrho_2(s)}{\sqrt{v^*}\varrho_4}, \quad (56d)$$

$$\begin{aligned} \Gamma_7(s) = & \frac{\tilde{m}g\chi\alpha v^*\varrho_4(\varrho_1(s) + \varrho_2(s) - 2\Gamma_1(s))}{\varrho_3} \\ & + \frac{\tilde{m}g\chi\sqrt{v^*}(2\alpha\gamma v^* - 2\psi)(\varrho_1(s) - \varrho_2(s))}{\varrho_3}, \end{aligned} \quad (56e)$$

$$\Gamma_8(s) = \frac{\psi\sqrt{v^*}(\varrho_1(s) - \varrho_2(s))}{\varrho_4}, \quad (56f)$$

$$\Gamma_9(s) = \frac{\varrho_4(\varrho_1(s) + \varrho_2(s)) + \gamma\sqrt{v^*}(\varrho_1(s) - \varrho_2(s))}{2\varrho_4}, \quad (56g)$$

with

$$\varrho_1(s) = \exp\left(\frac{(\varrho_4 + \gamma\sqrt{v^*})s}{2\sqrt{v^*}}\right), \quad (57a)$$

$$\varrho_2(s) = \exp\left(\frac{(\varrho_4 - \gamma\sqrt{v^*})s}{2\sqrt{v^*}}\right), \quad (57b)$$

$$\varrho_3 = 2\varrho_4[v^*\alpha(\alpha - \gamma) + \psi], \quad (57c)$$

$$\varrho_4 = \sqrt{\gamma^2 v^* - 4\psi}. \quad (57d)$$

Similarly, the time-dependent, conditional covariance matrix is formally given by $\boldsymbol{\Sigma}(s_F - s_0)$. More concretely, the following relationships may be deduced for the entries of $\boldsymbol{\Sigma}(s)$:

$$\boldsymbol{\Sigma}(s) = \begin{bmatrix} \Sigma_{YY}(s) & \Sigma_{Y\tilde{X}}(s) & \Sigma_{Y\tilde{V}}(s) \\ \Sigma_{\tilde{X}Y}(s) & \Sigma_{\tilde{X}\tilde{X}}(s) & \Sigma_{\tilde{X}\tilde{V}}(s) \\ \Sigma_{\tilde{V}Y}(s) & \Sigma_{\tilde{V}\tilde{X}}(s) & \Sigma_{\tilde{V}\tilde{V}}(s) \end{bmatrix}, \quad (58)$$

with

$$\Sigma_{YY}(s) = \frac{\beta^2}{2\alpha}(1 - e^{-2\alpha s}), \quad (59a)$$

$$\Sigma_{Y\tilde{X}}(s) = \Sigma_{\tilde{X}Y}(s) = \varsigma_2(s), \quad (59b)$$

$$\Sigma_{Y\tilde{V}}(s) = \Sigma_{\tilde{V}Y}(s) = \varsigma_3(s), \quad (59c)$$

$$\Sigma_{\tilde{X}\tilde{X}}(s) = -\int_0^s \left(\frac{\beta^2 \varsigma_6^2(s')}{\varsigma_4} + \frac{\eta^2(\varsigma_{10}(s') - \varsigma_{11}(s'))^2}{v^* \varsigma_8} \right) ds', \quad (59d)$$

$$\Sigma_{\tilde{X}\tilde{V}}(s) = \Sigma_{\tilde{V}\tilde{X}}(s) = \varsigma_1(s), \quad (59e)$$

$$\Sigma_{\tilde{V}\tilde{V}}(s) = -\int_0^s \left(\frac{\beta^2 \varsigma_7^2(s')}{\varsigma_4} + \frac{\eta^2 \varsigma_5^2(s')}{4\varsigma_8} \right) ds', \quad (59f)$$

where

$$\begin{aligned} \varsigma_1(s) = & \int_0^s \frac{\beta^2 \varsigma_7(s') \varsigma_6(s')}{\varsigma_4} ds' \\ & + \int_0^s \frac{\eta^2(\varsigma_{10}(s') - \varsigma_{11}(s')) \varsigma_5(s')}{2\sqrt{v^*} \varsigma_8} ds', \end{aligned} \quad (60a)$$

$$\varsigma_2(s) = -\int_0^s \frac{\beta^2 e^{-\alpha s'} \varsigma_6(s')}{2\varsigma_{12} \varsigma_9} ds', \quad (60b)$$

$$\varsigma_3(s) = \int_0^s \frac{\beta^2 e^{-\alpha s'} \varsigma_7(s')}{2\varsigma_{12}\varsigma_9} ds', \quad (60c)$$

$$\varsigma_4 = 4\varsigma_8\varsigma_9^2, \quad (60d)$$

$$\varsigma_5(s) = \varsigma_{12}(s)(\varsigma_{10}(s) + \varsigma_{11}(s)) + \gamma\sqrt{v^*}(\varsigma_{10}(s) - \varsigma_{11}(s)), \quad (60e)$$

$$\begin{aligned} \varsigma_6(s) = & \tilde{m}g\chi\varsigma_{12}(\varsigma_{10}(s) + \varsigma_{11}(s) - 2e^{-\alpha s}) \\ & + \tilde{m}g\chi\sqrt{v^*}(2\alpha - \gamma)(\varsigma_{10}(s) - \varsigma_{11}(s)), \end{aligned} \quad (60f)$$

$$\begin{aligned} \varsigma_7(s) = & \alpha\tilde{m}g\chi v^*\varsigma_{12}(\varsigma_{10}(s) + \varsigma_{11}(s) - 2e^{-\alpha s}) \\ & + \tilde{m}g\chi\sqrt{v^*}(\alpha\gamma v^* - 2\psi)(\varsigma_{10}(s) - \varsigma_{11}(s)), \end{aligned} \quad (60g)$$

$$\varsigma_8 = 4\psi - \gamma^2 v^*, \quad (60h)$$

$$\varsigma_9 = \alpha v^*(\alpha - \gamma) + \psi, \quad (60i)$$

$$\varsigma_{10}(s) = \exp\left(\frac{\varsigma_{12} + \gamma\sqrt{v^*}}{2\sqrt{v^*}}s\right), \quad (60j)$$

$$\varsigma_{11}(s) = \exp\left(\frac{\varsigma_{12} - \gamma\sqrt{v^*}}{2\sqrt{v^*}}s\right), \quad (60k)$$

$$\varsigma_{12} = \sqrt{\gamma^2 v^* - 4\psi}. \quad (60l)$$

Moreover, the eigenvalues of the matrix Γ , defined as in (54a), may be calculated as

$$\lambda_1 = \alpha, \quad (61a)$$

$$\lambda_2 = -\frac{\sqrt{\gamma^2 v^* - 4\psi} + \gamma\sqrt{v^*}}{2\sqrt{v^*}}, \quad (61b)$$

$$\lambda_3 = \frac{\sqrt{\gamma^2 v^* - 4\psi} - \gamma\sqrt{v^*}}{2\sqrt{v^*}}. \quad (61c)$$

A quick inspection of (61) reveals the existence of a stationary distribution also for the Ornstein-Uhlenbeck process described by (52). The stationary or limiting mean and covariance matrix, whose expressions are not explicitly reported in this paper, may hence be deduced directly from the conditional ones, by taking the limits $s_F, s \rightarrow \infty$. In this context, it should be also clarified that the integrals appearing in (60a), (60b), and (60c) may be evaluated analytically, albeit yielding extremely lengthy expressions which are ultimately too cumbersome to implement.

Starting with the results derived above, the propulsive force may be calculated again according to (38), where the constant term b_k reads as in (39c), but $\mathbf{A}_k \triangleq \mathbf{A}_{kp} + \mathbf{A}_{kI} + \mathbf{A}_{kD}$, with

$$\mathbf{A}_{kp} = -k_p \begin{bmatrix} 0 & 0 & 1 \end{bmatrix}, \quad (62a)$$

$$\mathbf{A}_{kI} = -k_I \begin{bmatrix} 0 & 1 & 0 \end{bmatrix}, \quad (62b)$$

$$\mathbf{A}_{kD} = -v^* k_D \begin{bmatrix} \tilde{m}g\chi & -\psi & -\gamma \end{bmatrix}. \quad (62c)$$

Finally, the expressions for the propulsive force required at the wheel level, the energy, and the energy consumption may

be deduced to be formally identical to those reported in Section III-C; their derivation is not repeated.

DECLARATION OF INTEREST

Declaration of interest: none.

STATEMENT OF CONTRIBUTIONS

Luigi Romano: Conceptualization, Data curation, Theory, Formal analysis, Investigation, Methodology, Software, Validation, Visualization, Writing – original draft; **Krzysztof Podgórski:** Theory, Methodology; **Carl Emvin:** Software; **Pär Johannesson:** Funding acquisition; **Jonas Fredriksson:** Funding acquisition, Project administration; **Fredrik Bruzelius:** Funding acquisition, Project administration. All the authors read and approved the original version of the manuscript.

REFERENCES

- [1] Z. Hausfather, “State of the climate: 2020 set to be the first OT second warmest year on record,” 2020. [Online]. Available: <https://www.carbonbrief.org/state-of-the-climate-2020-set-to-be-first-or-second-warmest-year-on-record>
- [2] J. Cook et al., “Quantifying the consensus on anthropogenic global warming in the scientific literature,” *Environ. Res. Lett.*, vol. 8, no. 2, 2013, Art. no. 024024, doi: [10.1088/1748-9326/8/2/024024](https://doi.org/10.1088/1748-9326/8/2/024024).
- [3] R. S. J. Tol, “Quantifying the consensus on anthropogenic global warming in the literature: A re-analysis,” *Energy Policy*, vol. 73, pp. 701–705, 2014. [Online]. Available: <https://www.sciencedirect.com/science/article/pii/S0301421514002821>
- [4] S. Callery, “Climate change: How do we know,” Two independence square, Washington, DC, USA, Tech. Rep., 2019.
- [5] Union of Concerned Scientists, “Global warming,” Cambridge, MA, USA, Tech. Rep., 2019.
- [6] European Environmental Agency, “Greenhouse gas emissions from transport,” Tech. Rep., 2019.
- [7] C. C. C. Service, “Record-breaking temperatures for june!,” 2019. [Online]. Available: <https://ucsusa.org/climate/science>
- [8] U. S. E. P. Agency, “Overview of greenhouse gases,” Environmental Protection Agency, Two independence square, Washington DC, USA, 2019.
- [9] Eurostat, “Greenhouse gas emission statistics—emission inventories,” 2019. [Online]. Available: https://ec.europa.eu/eurostat/statistics-explained/index.php/Greenhouse_gas_emission_statistics
- [10] G. C. Project, “The global carbon atlas, CO₂ emissions,” 2017. [Online]. Available: <http://www.globalcarbonatlas.org/en/CO2-emissions>
- [11] European Commission, “Regulation (EU) no 333/2014 of the european parliament and of the council of 11 march 2014 amending regulation (EC) no 443/2009 to define modalities for reaching the 2020 target to reduce CO₂ emissions from new passenger cars,” 2014. [Online]. Available: <https://eur-lex.europa.eu/legal-content/EN/TXT/?uri=OJ%3AL%3A2014%3A084%3ATOC>
- [12] European Commission, “Regulation (EU) no 253/2014 of the european parliament and of the council of 26 february 2014 amending regulation (EC) no 510/2011 to define modalities for reaching the 2020 target to reduce CO₂ emissions from new light commercial vehicles,” 2014. [Online]. Available: <https://eur-lex.europa.eu/legal-content/EN/TXT/?uri=OJ%3AL%3A2014%3A084%3ATOC>
- [13] European Commission, “Commission regulation (EU) no 2017/2400,” *Official J. Eur. Union*, 60.1 247, 2017. [Online]. Available: <https://eur-lex.europa.eu/legal-content/EN/TXT/?uri=OJ%3AL%3A2017%3A349%3ATOC>
- [14] European Commission, “Vehicle energy consumption calculation tool—VECTO,” 2019. [Online]. Available: https://ec.europa.eu/clima/policies/transport/vehicles/vecto_en
- [15] L. Guzzella and A. Sciarretta, *Vehicle Propulsion Systems: Introduction to Modeling and Optimization*, 3rd ed. Berlin, Germany: Springer, 2013, doi: [10.1007/978-3-642-35913-2](https://doi.org/10.1007/978-3-642-35913-2).

- [16] U. Kiencke and L. Nielsen, *Automotive Control Systems*, 2nd ed. Berlin, Heidelberg: Springer, 2005, doi: [10.1007/b137654](https://doi.org/10.1007/b137654).
- [17] European Commission, "Vehicle energy consumption calculation tool – VECTO," 2019. [Online]. Available: https://ec.europa.eu/clima/policies/transport/vehicles/veccto_en
- [18] D. W. Wyatt, H. Li, and J. E. Tate, "The impact of road grade on carbon dioxide (CO₂) emissions of passenger vehicle in real-world driving," *Transp. Res. Part D: Transport Environ.*, vol. 32, pp. 160–170, 2014, doi: [10.1016/j.trd.2014.07.015](https://doi.org/10.1016/j.trd.2014.07.015).
- [19] K. Sentoff, L. Aultman-Hall, and B. Holmé, "Implications of driving style on road grade for accurate vehicle data and emissions estimates," *Transp. Res. Part D: Transport Environ.*, vol. 35, pp. 175–188, 2015, doi: [10.1016/j.trd.2014.11.021](https://doi.org/10.1016/j.trd.2014.11.021).
- [20] D. Llopis-Castelló, A. M. Pérez-Zuriaga, F. J. Camacho-Torregrosa, and A. García, "Impact of horizontal geometric design of two-lane rural roads on vehicle CO₂ emissions," *Transp. Res. Part D: Transport Environ.*, vol. 59, pp. 46–57, 2018, doi: [10.1016/j.trd.2017.12.020](https://doi.org/10.1016/j.trd.2017.12.020).
- [21] A. Sciarretta, *Energy-Efficient Driving of Road Vehicles*, 1st ed. Cham, Switzerland: Springer, 2020, doi: [10.1007/978-3-030-24127-8](https://doi.org/10.1007/978-3-030-24127-8).
- [22] T. Lee, B. Adornato, and Z. S. Filipi, "Synthesis of real-world driving cycles and their use for estimating PHEV energy consumption and charging opportunities: Case study for midwest/U.S.," *IEEE Trans. Veh. Technol.*, vol. 60, no. 9, pp. 4153–4163, Nov. 2011, doi: [10.1109/TVT.2011.2168251](https://doi.org/10.1109/TVT.2011.2168251).
- [23] G. Amirjamshidi and M. J. Roorda, "Development of simulated driving cycles for light, medium, and heavy duty trucks: Case of the Toronto waterfront area," *Transp. Res. Part D: Transport Environ.*, vol. 34, pp. 255–266, 2015, doi: [10.1016/j.trd.2014.11.010](https://doi.org/10.1016/j.trd.2014.11.010).
- [24] S. H. Kamble, T. V. Mathew, and G. K. Sharma, "Development of real-world driving cycle: Case study of Pune, India," *Transp. Res. Part D: Transport Environ.*, vol. 14, no. 2, pp. 132–140, 2009, doi: [10.1016/j.trd.2008.11.008](https://doi.org/10.1016/j.trd.2008.11.008).
- [25] E. Silvas, K. Hereijgers, H. Peng, T. Hofman, and M. Steinbuch, "Synthesis of realistic driving cycles with high accuracy and computational speed, including slope information," *IEEE Trans. Veh. Technol.*, vol. 65, no. 6, pp. 4118–4121, Jun. 2016, doi: [10.1109/TVT.2016.2546338](https://doi.org/10.1109/TVT.2016.2546338).
- [26] W. T. Hung, H. Y. Tong, C. P. Lee, K. Ha, and L. Y. Pao, "Development of a practical driving cycle construction methodology: A case study in Hong Kong," *Transp. Res. Part D: Transport Environ.*, vol. 12, no. 2, pp. 115–128, 2007, doi: [10.1016/j.trd.2007.01.002](https://doi.org/10.1016/j.trd.2007.01.002).
- [27] Y. Sun, Y. Hu, H. Zhang, F. Wang, and H. Chen, "A parallel supervision system for vehicle CO₂ emissions based on OBD-independent information," *IEEE Trans. Intell. Veh.*, vol. 8, no. 3, pp. 2077–2087, Mar. 2023, doi: [10.1109/TIV.2022.3210283](https://doi.org/10.1109/TIV.2022.3210283).
- [28] D. T. Machacek, K. Barhoumi, J. M. Ritzmann, T. Huber, and C. H. Onder, "Multi-level model predictive control for the energy management of hybrid electric vehicles including thermal derating," *IEEE Trans. Veh. Technol.*, vol. 71, no. 10, pp. 10400–10414, Oct. 2022, doi: [10.1109/TVT.2022.3183866](https://doi.org/10.1109/TVT.2022.3183866).
- [29] F. Widmer, A. Ritter, P. Duhr, and C. H. Onder, "Energy and thermal management, IETMS, Optimal control and sizing, battery health, electric drivetrain, public transport," *eTransportation*, vol. 14, 2022, Art. no. 100196, doi: [10.1016/j.etrans.2022.100196](https://doi.org/10.1016/j.etrans.2022.100196).
- [30] E. Kamal and L. Adouane, "Intelligent energy management strategy based on artificial neural fuzzy for hybrid vehicle," *IEEE Trans. Intell. Veh.*, vol. 3, no. 1, pp. 112–125, Mar. 2018, doi: [10.1109/TIV.2017.2788185](https://doi.org/10.1109/TIV.2017.2788185).
- [31] W. D. Connor, Y. Wang, A. A. Malikopoulos, S. G. Advani, and A. K. Prasad, "Impact of connectivity on energy consumption and battery life for electric vehicles," *IEEE Trans. Intell. Veh.*, vol. 6, no. 1, pp. 14–23, Mar. 2021, doi: [10.1109/TIV.2020.3032642](https://doi.org/10.1109/TIV.2020.3032642).
- [32] C. Yang, R. Chen, W. Wang, Y. Li, X. Shen, and C. Xiang, "Cyber-physical optimization-based fuzzy control strategy for plug-in hybrid electric buses using iterative modified particle swarm optimization," *IEEE Trans. Intell. Veh.*, vol. 8, no. 5, pp. 3285–3298, May 2023, doi: [10.1109/TIV.2023.3260007](https://doi.org/10.1109/TIV.2023.3260007).
- [33] T. Liu, K. Tan, W. Zhu, and L. Feng, "Computationally efficient energy management for a parallel hybrid electric vehicle using adaptive dynamic programming," *IEEE Trans. Intell. Veh.*, vol. 9, no. 2, pp. 4085–4099, Feb. 2024, doi: [10.1109/TIV.2023.3285392](https://doi.org/10.1109/TIV.2023.3285392).
- [34] H. Zhang, N. Lei, and Z. Wang, "Ammonia-hydrogen propulsion system for carbon-free heavy-duty vehicles," *Appl. Energy*, vol. 369, 2024, Art. no. 123505, doi: [10.1016/j.apenergy.2024.123505](https://doi.org/10.1016/j.apenergy.2024.123505).
- [35] N. Lei, H. Zhang, R. Li, J. Yu, H. Wang, and Z. Wang, "Physics-informed data-driven modeling approach for commuting-oriented hybrid powertrain optimization," *Energy Convers. Manage.*, vol. 299, 2024, Art. no. 117814, doi: [10.1016/j.enconman.2023.117814](https://doi.org/10.1016/j.enconman.2023.117814).
- [36] H. Zhang, N. Lei, S. Liu, Q. Fan, and Z. Wang, "Data-driven predictive energy consumption minimization strategy for connected plug-in hybrid electric vehicles," *Energy*, vol. 283, 2023, Art. no. 128514, doi: [10.1016/j.energy.2023.128514](https://doi.org/10.1016/j.energy.2023.128514).
- [37] H. Zhang, B. Chen, N. Lei, B. Li, R. Li, and Z. Wang, "Integrated thermal and energy management of connected hybrid electric vehicles using deep reinforcement learning," *IEEE Trans. Transport. Electrification*, vol. 10, no. 2, pp. 4594–4603, Jun. 2024, doi: [10.1109/TTE.2023.3309396](https://doi.org/10.1109/TTE.2023.3309396).
- [38] M. Shen, R. A. Dollar, T. G. Molnar, C. R. He, A. Vahidi, and G. Orosz, "Energy-efficient reactive and predictive connected cruise control," *IEEE Trans. Intell. Veh.*, vol. 9, no. 1, pp. 944–957, Jan. 2024, doi: [10.1109/TIV.2023.3281763](https://doi.org/10.1109/TIV.2023.3281763).
- [39] P. Nyberg, E. Frisk, and L. Nielsen, "Using real-world driving databases to generate driving cycles with equivalence properties," *IEEE Trans. Veh. Technol.*, vol. 65, no. 6, pp. 4095–4105, Jun. 2016, doi: [10.1109/TVT.2015.2502069](https://doi.org/10.1109/TVT.2015.2502069).
- [40] P. Nyberg, E. Frisk, and L. Nielsen, "Driving cycle equivalence and transformation," *IEEE Trans. Veh. Technol.*, vol. 66, no. 3, pp. 1963–1974, Mar. 2017, doi: [10.1109/TVT.2016.2582079](https://doi.org/10.1109/TVT.2016.2582079).
- [41] K. Kivekäs, J. Vepsäläinen, and K. Tammi, "Stochastic driving cycle synthesis for analyzing the energy consumption of a battery electric bus," *IEEE Access*, vol. 6, pp. 55586–55598, 2018, doi: [10.1109/ACCESS.2018.2871574](https://doi.org/10.1109/ACCESS.2018.2871574).
- [42] K. Kivekäs, J. Vepsäläinen, K. Tammi, and J. Anttila, "Influence of driving cycle uncertainty on electric city bus energy consumption," in *2017 IEEE Veh. Power Propulsion Conf.*, 2017, pp. 1–5, doi: [10.1109/VPPC.2017.8331014](https://doi.org/10.1109/VPPC.2017.8331014).
- [43] P. Pettersson, S. Berglund, B. J. Jacobson, L. Fast, P. Johannesson, and F. Santandrea, "A proposal for an operating cycle description format for road transport missions," *Eur. Transport Res. Rev.*, vol. 10, no. 31, pp. 1–19, 2013, doi: [10.1186/s12544-018-0298-4](https://doi.org/10.1186/s12544-018-0298-4).
- [44] P. Pettersson, P. Johannesson, B. Jacobson, F. Bruzelius, L. Fast, and S. Berglund, "A statistical operating cycle description for prediction of road vehicles' energy consumption," *Transp. Res. Part D: Transport Environ.*, vol. 73, pp. 205–229, 2013, doi: [10.1016/j.trd.2019.07.006](https://doi.org/10.1016/j.trd.2019.07.006).
- [45] L. Romano, P. Johannesson, F. Bruzelius, and B. Jacobson, "An enhanced stochastic operating cycle description including weather and traffic models," *Transp. Res. Part D: Transport Environ.*, vol. 97, 2013, Art. no. 102878, doi: [10.1016/j.trd.2021.102878](https://doi.org/10.1016/j.trd.2021.102878).
- [46] L. Romano, C. Emvin, F. Bruzelius, P. Johannesson, R. Andersson, and B. Jacobson, "Stochastic modeling of mission stops and variable cargo weight for heavy-duty trucks," in *2023 IEEE Veh. Power Propulsion Conf.*, 2023, pp. 1–8.
- [47] L. Romano, P. Johannesson, E. Nordström, F. Bruzelius, R. Andersson, and B. Jacobson, "A classification method of road transport missions and applications using the operating cycle format," *IEEE Access*, vol. 10, pp. 73087–73121, 2022, doi: [10.1109/ACCESS.2022.3188872](https://doi.org/10.1109/ACCESS.2022.3188872).
- [48] L. Romano, M. Godio, P. Johannesson, F. Bruzelius, T. Ghandriz, and B. Jacobson, "Development of the Västra Götaland operating cycle for long-haul heavy-duty vehicles," *IEEE Access*, vol. 11, pp. 73268–73302, 2023, doi: [10.1109/ACCESS.2023.3295989](https://doi.org/10.1109/ACCESS.2023.3295989).
- [49] A. Godet, J. N. Nurup, J. T. Saber, G. Panagakos, and M. B. Barfod, "Operational cycles for maritime transportation: A benchmarking tool for ship energy efficiency," *Transp. Res. Part D: Transport Environ.*, vol. 121, 2023, Art. no. 103840, doi: [10.1016/j.trd.2023.103840](https://doi.org/10.1016/j.trd.2023.103840).
- [50] L. Romano, "The operating cycle representation of road transport missions," Doctoral thesis, Chalmers Univ. Technol., Gothenburg, Sweden, 2023.
- [51] T. Ghandriz, B. Jacobson, L. Laine, and J. Hellgren, "Impact of automated driving systems on road freight transport and electrified propulsion of heavy vehicles," *Transp. Res. Part C: Emerg. Technol.*, vol. 115, 2020, Art. no. 102610, doi: [10.1016/j.trc.2020.102610](https://doi.org/10.1016/j.trc.2020.102610).
- [52] A. Kolmogoroff, "Über die analytischen methoden in der wahrscheinlichkeitsrechnung," *Math. Ann.*, vol. 104, pp. 415–458, 1931, doi: [10.1007/BF01457949](https://doi.org/10.1007/BF01457949).
- [53] A. D. Fokker, "Die mittlere Energie rotierender elektrischer dipole im strahlungsfeld," *Ann. Phys.*, vol. 348, pp. 810–820, 1914, doi: [10.1002/andp.19143480507](https://doi.org/10.1002/andp.19143480507).
- [54] M. Planck, "Über einen satz der statistischen dynamik und seine erweiterung in der quantentheorie," *Sitzungsberichte der Preussischen Akademie der Wissenschaften zu Berlin*, vol. 24, pp. 324–341, 1917.
- [55] H. Risken, *The Fokker-Planck Equation: Methods of Solution and Applications*, 2nd ed. Berlin/Heidelberg, Germany: Springer, 1996, doi: [10.1007/978-3-642-61544-3](https://doi.org/10.1007/978-3-642-61544-3).

- [56] A. Einstein, "Über die von der molekularkinetischen theorie der wärme geforderte bewegung von in ruhenden flüssigkeiten suspendierten teilchen," *Ann. Phys.*, vol. 322, pp. 549–560, 1905, doi: [10.1002/andp.19053220806](#).
- [57] Y. Mardoukhi et al., "Spurious ergodicity breaking in normal and fractional Ornstein–Uhlenbeck process," *New J. Phys.*, vol. 22, 2020, Art. no. 073012, doi: [10.1088/1367-2630/ab950b](#).
- [58] D. Sornette, "Fokker–Planck equation of distributions of financial returns and power laws," *Physica A: Stat. Mechanics Appl.*, vol. 290, no. 1–2, pp. 211–217, 2001, doi: [10.1016/S0378-4371\(00\)00571-9](#).
- [59] B. N. J. Persson, "Theory of rubber friction and contact mechanics," *J. Chem. Phys.*, vol. 115, no. 8, pp. 3840–3861, 2001, doi: [10.1063/1.1388626](#).
- [60] B. N. J. Persson, O. Albohr, U. Tartaglino, A. I. Volokitin, and E. Tosatti, "On the nature of surface roughness with application to contact mechanics, sealing, rubber friction and adhesion," *J. Phys.: Condens. Matter*, vol. 17, no. 1, pp. R1–R62, 2004.
- [61] G. Carbone et al., "Contact mechanics and rubber friction for randomly rough surfaces with anisotropic statistical properties," *Eur. Phys. J. E*, vol. 29, pp. 275–284, 2009, doi: [10.1140/epje/i2009-10484-8](#).
- [62] I. G. Goryacheva, *Contact Mechanics in Tribology*, 1st ed. Dordrecht, The Netherlands: Springer, 1998, doi: [10.1007/978-94-015-9048-8](#).
- [63] G. Heinrich and M. Klüppel, "Rubber friction, tread deformation and tire traction," *Wear*, vol. 265, no. 7/8, pp. 1052–1060. [Online]. Available: <https://www.sciencedirect.com/science/article/pii/S0043164808000847>
- [64] P. Pettersson, B. Jacobson, F. Bruzelius, P. Johannesson, and L. Fast, "Intrinsic differences between backward and forward vehicle simulation models," *IFAC-PapersOnLine*, vol. 53, no. 2, pp. 14292–14299, 2020, doi: [10.1016/j.ifacol.2020.12.1368](#).
- [65] Y. B. Khoo, C. H. Wang, P. Paevere, and A. Higgins, "Statistical modeling of Electric Vehicle electricity consumption in the Victorian EV Trial, Australia," *Transp. Res. Part D: Transport Environ.*, vol. 32, pp. 263–277, 2014, doi: [10.1016/j.trd.2014.08.017](#).
- [66] A. Capiello, I. Chabini, E. K. Nam, A. Lue, and M. A. Zeid, "A statistical model of vehicle emissions and fuel consumption," in *Proc. IEEE 5th Int. Conf. Intell. Transp. Syst.*, 2002, pp. 801–809, doi: [10.1109/ITSC.2002.1041322](#).
- [67] P. Pettersson, "Operating cycle representations for road vehicles," Doctoral dissertation, Chalmers University of Technology, Gothenburg, Sweden, 2019.
- [68] T. Ghandriz, "Transportation mission-based optimization of heavy combination road vehicles and distributed propulsion, including predictive energy and motion control," Doctoral dissertation, Chalmers Univ. Technol., Gothenburg, Sweden, 2020.
- [69] C. Beckers, I. Besselink, and H. Nijmeijer, "Assessing the impact of cornering losses on the energy consumption of electric city buses," *Transp. Res. Part D: Transport Environ.*, vol. 86, pp. 1361–9209, 2021, doi: [10.1109/VPPC53923.2021.9699205](#).
- [70] F. C. Klebaner, *Introduction to Stochastic Calculus With Applications*, 3rd ed. London, U.K.: Imperial College Press, 2012.
- [71] B. Øksendal, *Stochastic Differential Equations: An Introduction With Applications*, 6th ed. Berlin/Heidelberg, Germany: Springer, 2003, doi: [10.1007/978-3-642-14394-6](#).
- [72] A. Bezen and F. C. Klebaner, "Stationary solutions and stability of second order random differential equations," *Physica A: Stat. Mechanics Appl.*, vol. 233, no. 3–4, pp. 809–823, 1996, doi: [10.1016/S0378-4371\(96\)00205-1](#).
- [73] V. Milanés, S. E. Shladover, J. Spring, C. Nowakowski, H. Kawazoe, and M. Nakamura, "Cooperative adaptive cruise control in real traffic situations," *IEEE Trans. Intell. Transp. Syst.*, vol. 15, pp. 296–305, Feb. 2014, doi: [10.1109/TITS.2013.2278494](#).
- [74] A. Kesting, M. Treiber, and D. Helbing, "Enhanced intelligent driver model to access the impact of driving strategies on traffic capacity," *Philos. Trans. Roy. Soc. A: Math., Phys. Eng. Sci.*, vol. 368, pp. 4585–4605, 2010, doi: [10.1098/rsta.2010.0084](#).
- [75] P. G. Gipps, "A behavioural car-following model for computer simulation," *Transp. Res. Part B: Methodological*, vol. 15, no. 2, pp. 105–111, 1981, doi: [10.1016/0191-2615\(81\)90037-0](#).
- [76] M. Makridis, G. Fontaras, G. B. Ciuffo, and K. Mattas, "MFC free-flow model: Introducing vehicle dynamics in microsimulation," *Transp. Res. Rec.*, vol. 2673, no. 4, pp. 762–777, 2019, doi: [10.1177/0361198119838515](#).
- [77] K. Fadhloun and H. Rakha, "A novel vehicle dynamics and human behavior car-following model: Model development and preliminary testing," *Int. J. Transp. Sci. Technol.*, vol. 9, pp. 14–28, 2019, doi: [10.1016/j.ijtst.2019.05.004](#).
- [78] B. Ciuffo, M. Makridis, T. Toledo, and G. Fontaras, "Capability of current car-following models to reproduce vehicle free-flow acceleration dynamics," *IEEE Trans. Intell. Transp. Syst.*, vol. 19, no. 11, pp. 3594–3603, Nov. 2018, doi: [10.1109/TITS.2018.2866271](#).
- [79] C. I. Chatzikomis and K. N. Spentzas, "A path-following driver model with longitudinal and lateral control of vehicle's motion," *Forschung im Ingenieurwesen*, vol. 73, no. 4, pp. 257–266, 2009, doi: [10.1007/s10010-009-0112-5](#).
- [80] Y. Ti, R. Wang, T. Song, and W. Zhao, "The study of a unified driver model controller based on fractional-order PI $\lambda D\mu$ and internal model control," *Proc. Inst. Mech. Engineers, Part D: J. Automobile Eng.*, vol. 237, no. 9, pp. 2374–2383, 2023, doi: [10.1177/0954407020964649](#).
- [81] P. Swethamarai and P. Lakshmi, "Design and implementation of fuzzy-PID controller for an active quarter car driver model to minimize driver body acceleration," in *2019 IEEE Int. Syst. Conf.*, Orlando, FL, USA, 2019, pp. 1–6, doi: [10.1109/SYSCON.2019.8836940](#).
- [82] C. C. MacAdam, "Application of an optimal preview control for simulation of closed-loop automobile driving," *IEEE Trans. Syst., Man, Cybern.*, vol. 11, no. 6, pp. 393–399, Jun. 1981.
- [83] C. C. MacAdam, "Development of driver/vehicle steering interaction models for dynamic analysis," Ann Arbor, Michigan, The University of Michigan Transportation Research Institute, Ann Arbor, MI, USA, Final Tech. Rep. UMTRI-88-53, Dec. 1988.
- [84] P. Johannesson, K. Podgórski, I. Rychlik, and N. Shariati, "AR(1) time series with autoregressive gamma variance for road topography modeling," *Probabilistic Eng. Mechanics*, vol. 34, pp. 106–116, 2016, doi: [10.1016/j.probengmech.2015.12.006](#).
- [85] P. Johannesson, K. Podgórski, and I. Rychlik, "Laplace distribution models for road topography and roughness," *Int. J. Veh. Perform.*, vol. 3, no. 3, pp. 224–258, 2017. [Online]. Available: <http://www.inderscience.com/offer.php?id=85032>
- [86] G. E. Uhlenbeck and L. S. Ornstein, "On the theory of the Brownian motion," *Phys. Rev.*, vol. 36, 1930, Art. no. 823, doi: [10.1103/PhysRev.36.823](#).
- [87] P. Vatiwutipong and N. Phewchean, "Alternative way to derive the distribution of the multivariate Ornstein–Uhlenbeck process," *Adv. Difference Equ.*, vol. 276, pp. 1–7, 2019, doi: [10.1186/s13662-019-2214-1](#).
- [88] G. B. Folland, *Real Analysis: Modern Techniques and Their Applications*, 2nd ed. Hoboken, NJ, USA: Wiley, 1999.



Luigi Romano (Member, IEEE) received the M.Sc. in mechanical engineering from the University of Naples "Federico II", Naples, Italy, in 2018, the Ph.D. degree in vehicle engineering from the Chalmers University of Technology, Gothenburg, Sweden, in 2023, and the second M.Sc. degree in applied mathematics from the University of Gothenburg, Gothenburg. Since 2024, he has been affiliated with the Vehicular Systems Group with the Department of Electrical Engineering, Linköping University, Linköping, Sweden, where he is a VR Postdoctoral Fellow funded by the Swedish Research Council. His primary research interests include the mathematical modeling and analysis of vehicular systems and components, with particular emphasis on pure road vehicle dynamics and energy-related aspects, as well as the development of control and estimation algorithms for automotive and transportation applications.



Krzysztof Podgórski received the Ph.D. degree in mathematics from the Wrocław University of Science and Technology, Wrocław, Poland, and the second Ph.D. degree in statistics from Michigan State University, East Lansing, MI, USA. His academic career has spanned several countries, including Poland, the USA, Ireland, and Sweden. He is currently a Professor of statistics and the Head of the Department of Statistics, Lund University's School of Economics and Management, Lund, Sweden. His research interests include stochastic processes in Gaussian and non-Gaussian settings, computationally intensive statistical methods, and their applications in mechanical engineering, environmental sciences, economics, and mathematical finance.



cycle format and the stochastic processes included. His research interests include residual range estimation, closely connected with energy consumption modeling.

Carl Emvin received the M.Sc. degree in systems, control and mechatronics from the Chalmers University of Technology, Gothenburg, Sweden, in 2023. He is currently working toward the Ph.D. degree with the Vehicle Dynamics Research Group, Department of Mechanics and Maritime Sciences, Chalmers University of Technology, Gothenburg, Sweden. During his studies and internship at Volvo Trucks, he became proficient in using and developing complete vehicle simulation models such as VehProp. During his master's thesis project, he contributed to the operating



experience in research and development in fatigue and load analysis with a focus on engineering statistics and reliability in industrial applications. He is the Co-editor of the handbook *Guide to Load Analysis for Durability in Vehicle Engineering*.

Pär Johannesson received the Ph.D. degree in mathematical statistics from the Lund Institute of Technology, Lund, Sweden, with a thesis on statistical load analysis for fatigue. He was a Postdoc in mathematical statistics with the Chalmers University of Technology, Gothenburg, Sweden, and PSA Peugeot Citroën, Paris, France. He is a docent in mathematical statistics at Chalmers. He is currently a Senior Researcher in mechanical reliability, fatigue, and load analysis. He has authored or coauthored more than 20 papers in international journals. He has more than 20 years of



Jonas Fredriksson received the M.Sc. degree in computer science engineering from the Lulea University of Technology, Lulea, Sweden, in 1997, and the Ph.D. degree in automatic control from the Chalmers University of Technology, Gothenburg, Sweden, in 2002. He is currently a Professor in mechatronics with the Department of Electrical Engineering at Chalmers. His research interests include modeling, control, and simulation, particularly in automotive applications.



estimation and control, tire modeling and simulation, driving simulators, and vehicle testing.

Fredrik Bruzelius received the M.Sc. degree in applied mathematics from Linköping University, Linköping, Sweden, and the Ph.D. degree in control theory from the Chalmers University of Technology, Gothenburg, Sweden, in 1999 and 2004, respectively. He worked for five years at Volvo developing vehicle dynamics estimation and control strategies in cars and trucks. He is currently a Senior Researcher in vehicle dynamics with the Department of Mechanics and Maritime Sciences, Chalmers University of Technology. His research interests include vehicle state